Reverberation Mapping of the Broad-Line Region in AGNs

Bradley M. Peterson
The Ohio State University

UFRGS Lectures

November 2013

Topics to be Covered

- *Lecture 1:* AGN properties and taxonomy, fundamental physics of AGNs, AGN structure
- *Lecture 2:* The broad-line region, emission-line variability, reverberation mapping principles, practice, and results, the radius–luminosity relationship, AGN outflows and disk-wind models
- *Lecture 3:* AGN luminosity function and its evolution, role of black holes, direct/indirect measurement of AGN black hole masses, relationships between BH mass and AGN/host properties, “industrial scale” reverberation mapping

The Broad-Line Region (BLR)

- Why focus on the BLR?
  - Closest to the central source,
    - Would be surprising if it is *not* involved in fueling the black hole.
  - Central black hole dominates kinematics, enabling measurement of black hole mass (Lecture 3).
- Difficulty: its angular size is only a few tens of microarcseconds, even in nearby AGNs.
  - Geometry/kinematics by reverberation mapping.

The Broad-Line Region

- 1000 ≤ FWHM ≤ 25,000 km s^{-1} ⇒ motion in deep potential?
  - $M \sim r\,\Delta V^2/G$
- Spectra ⇒ Photoionized gas at $T \approx 10^4$ K
- Absence of forbidden lines implies high density
  - But C III] λ1909 ⇒ $n_e < 10^{10}$ cm^{-3}

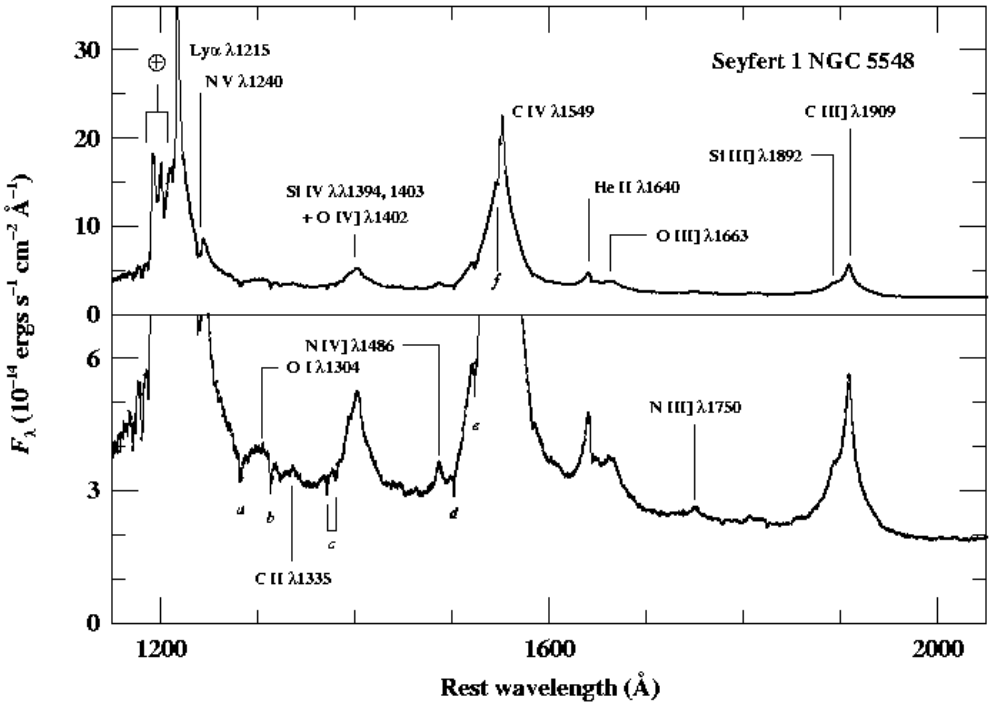

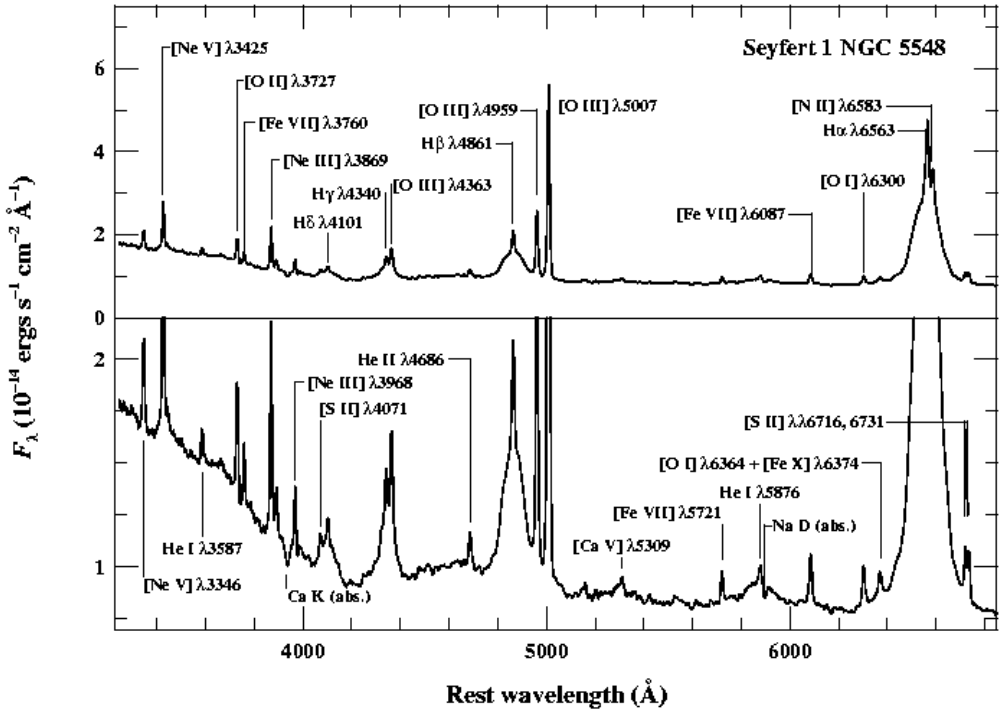

What is the BLR?

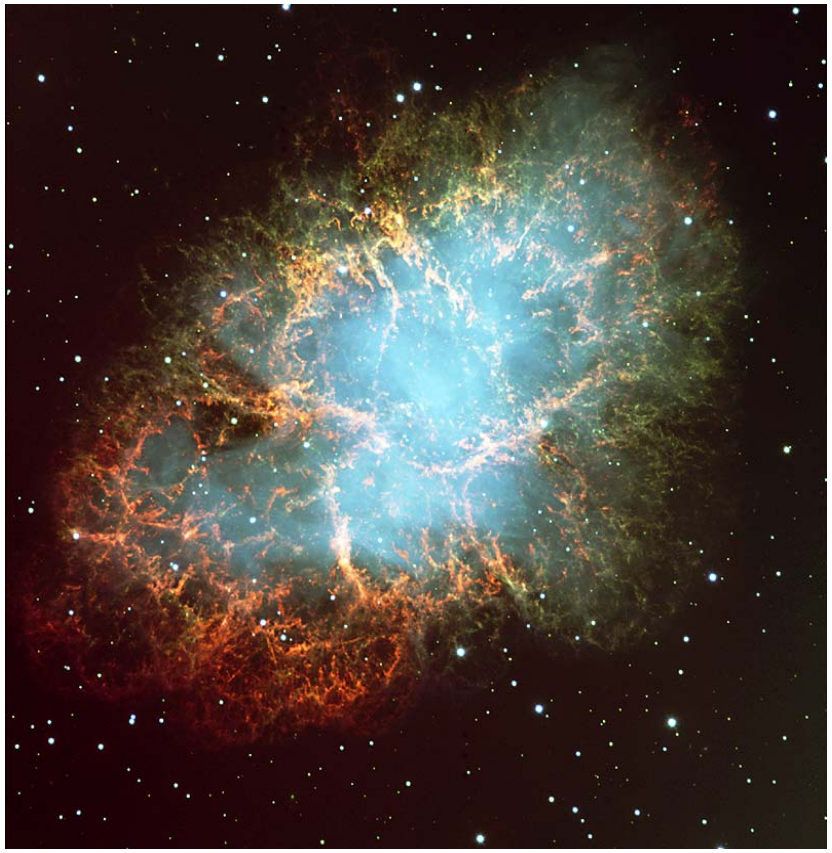

Crab Nebula
with VLT

- First notions based on Galactic nebulae, especially the Crab
  - system of “clouds” or “filaments.”
  - Ballistic or radiation-pressure driven outflow $\Rightarrow$ logarithmic profiles
  - Virial models implied very large masses
    - Early photoionization models overpredicted size of BLR (to be shown)

What is the BLR?

Flaw in the argument: emissivity per cloud is not proportional to cloud volume, but $N_c R_c^2 R_{Stromgren}$
Number and size not independently constrained.

Crab Nebula with VLT

- Number of clouds N_c of radius R_c:
  - Covering factor $\propto N_c R_c^2$
  - Line luminosity $\propto N_c R_c^3$
  - Combine these to find large number ($N_c > 10^8$) of small ($R_c \approx 10^{13}$ cm) clouds.
  - Combine size and density ($n_H \approx 10^{10}$ cm^{-3}), to get column density ($N_H \approx 10^{23}$ cm^{-2}), compatible with X-ray absorption.
  - Minimum mass of line-emitting material ~1$M_\odot$.

Large Number of Clouds?

- If clouds emit at thermal width (10 km/sec), then there must be a very large number of them to account for lack of small-scale structure in line profiles.

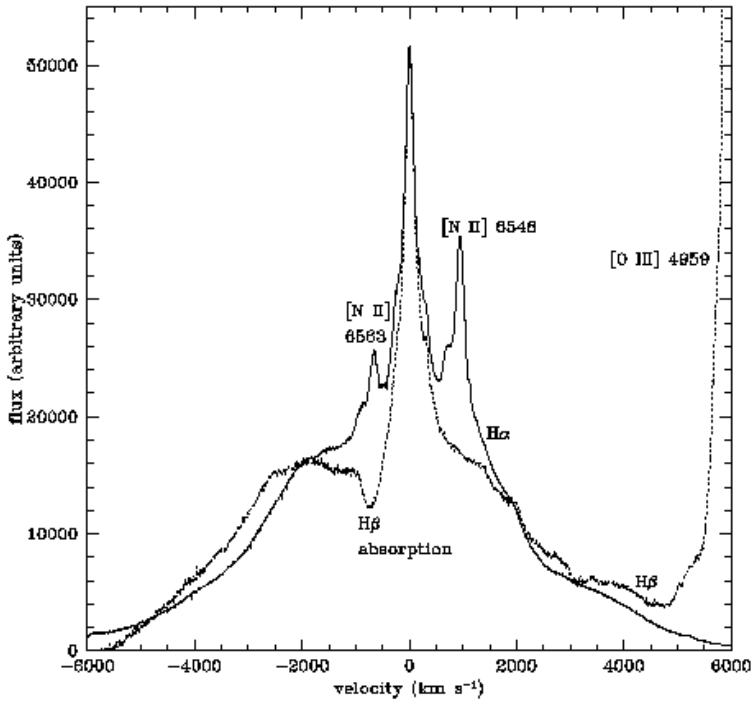

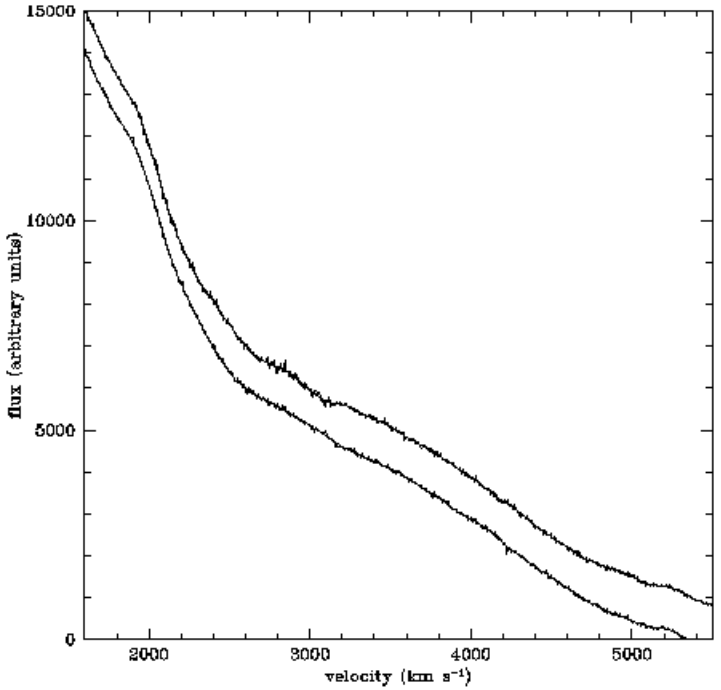

NGC 4151

Arav et al. (1998)

Photoionization Modeling of the BLR (circa 1982)

- In the 1970-80s, photoionization modeling was the best BLR probe.
- Single-cloud model:
  - Assume that C IV λ1549 and C III] λ1909 arise in same zone
  - Implies $n_e = 3 \times 10^9$ cm^{-3}
  - Line flux ratios then yield $U \approx 10^{-2}$

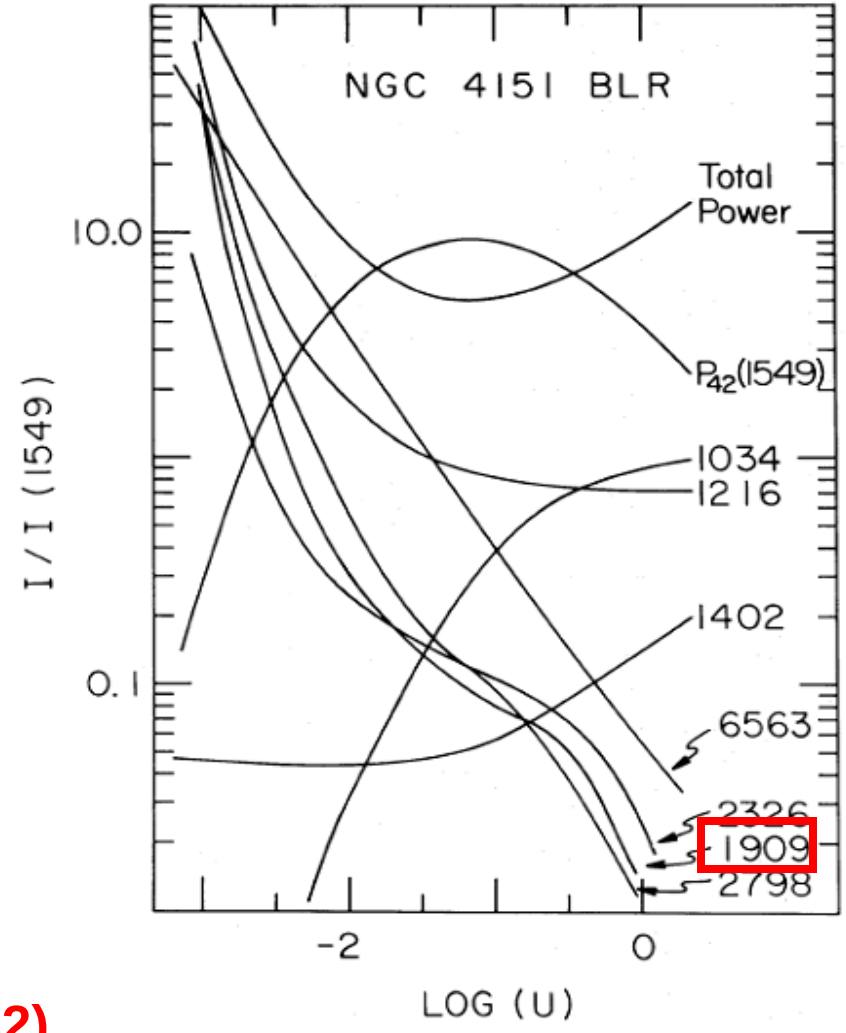

Ferland & Mushotzky (1982)

BLR Scaling with Luminosity

- To first order, AGN spectra look the same

$$U = \frac{Q(\mathrm{H})}{4\pi r^2 n_\mathrm{H} c} \propto \frac{L}{n_\mathrm{H} r^2}$$

$\Rightarrow$ Same ionization parameter U

$\Rightarrow$ Same density n_H

$$r \propto L^{1/2}$$

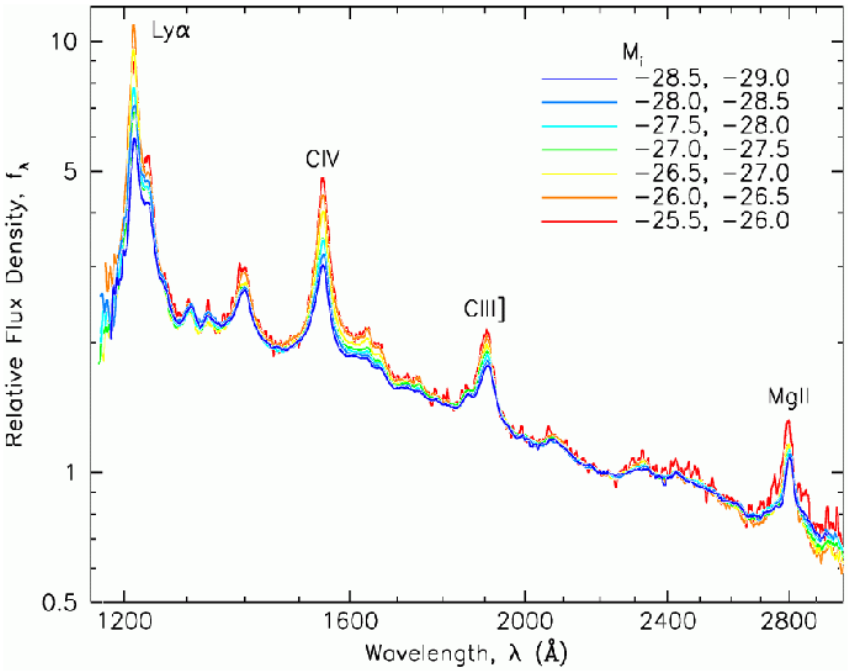

SDSS composites, by luminosity
Vanden Berk et al. (2004)

Predicting the Size of the BLR (for NGC 5548)

$$Q_{\rm ion}(H) = \int_{\nu_{\rm ion}}^{\infty} \frac{L_\nu}{h\nu}\, d\nu \approx 1.4\times10^{54}\ \text{photons s}^{-1}$$

$$r = \left(\frac{Q_{\rm ion}(H)}{4\pi c n_{\rm H} U} \right)^{1/2} \approx 3.3\times10^{17}\,\text{cm} \approx 130\,\text{light days}$$

This is an order of magnitude larger than determined by reverberation mapping!

Why Was Theory So Wrong?

- Incorrect assumption:
  - C IV and C III] are primarily produced at different radii.
  - Density in C IV emitting region is about 10^{11} cm^{-3}

Emission-Line Variability in Seyfert 1s

- Andrillat & Souffrin (1968) in NGC 3516
- Pastoriza & Gerola (1970) in NGC 1566

Photographic spectra reveal only extreme changes.

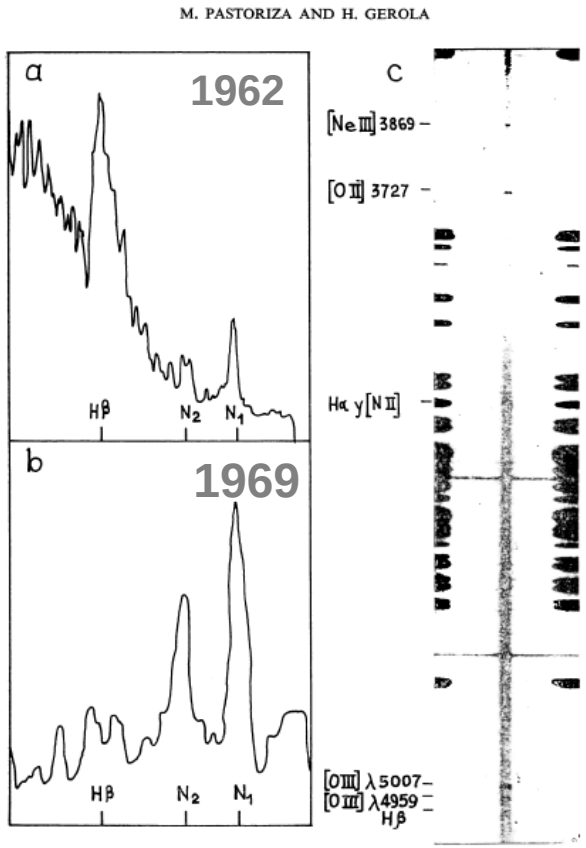

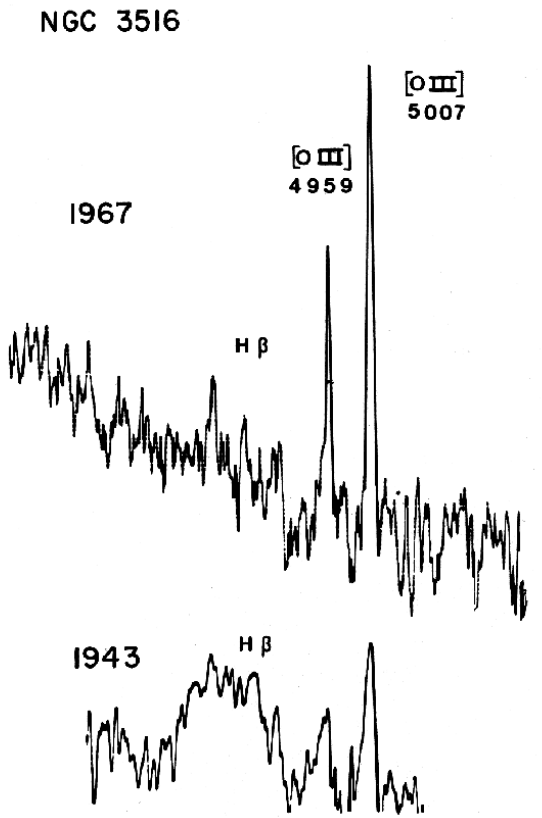

Andrillat & Souffrin 1968

Pastoriza & Gerola 1970

Emission-Line Variability

- Only very large changes could be detected photographically or with intensified television-type scanners (e.g., Image Dissector Scanners).
- Changes that were observed were often dramatic and reported as Seyferts “changing type” as broad components appeared or disappeared.

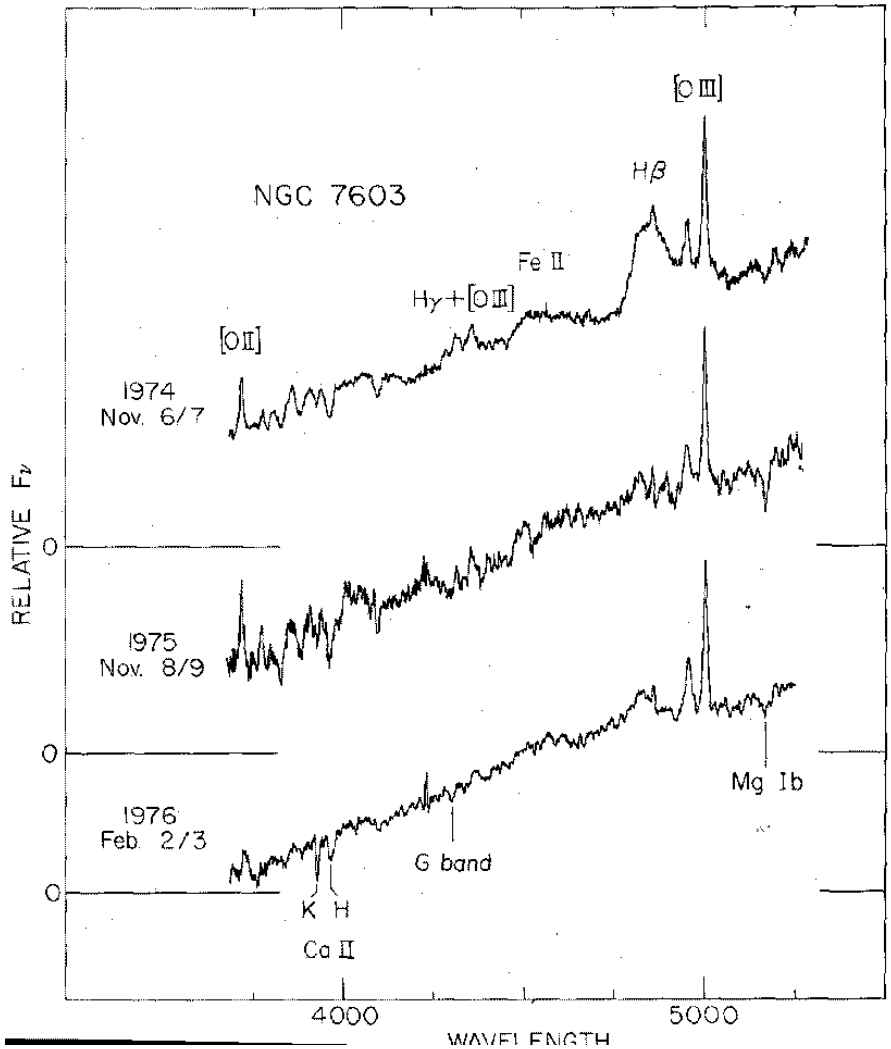

Tohline & Osterbrock 1976

Emission-Line Profile Variability

- Variability of broad emission-line profiles was detected in the early 1980s.
- This was originally thought to point to an ordered velocity field and propagation of excitation inhomogeneties.
- Led to development of reverberation mapping (seminal paper by Blandford & McKee 1982).

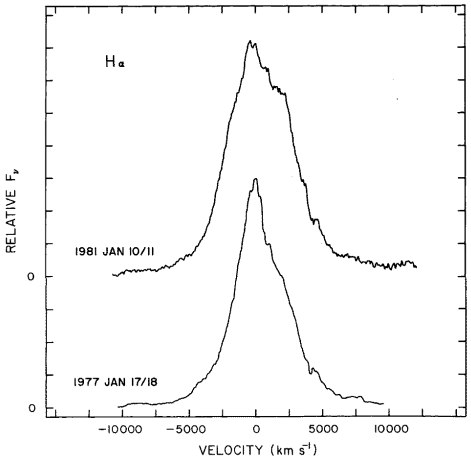

Foltz et al. 1981

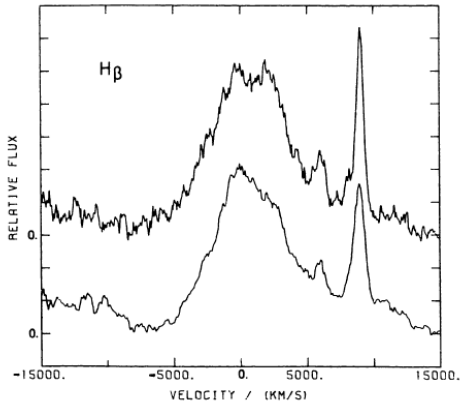

Kollatschny et al. 1981

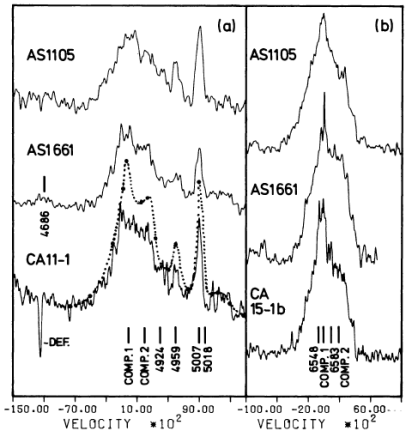

Schulz & Rafanelli 1981

First Monitoring Programs

- Made possible by existence of *International Ultraviolet Explorer* and proliferation of linear electronic detectors on moderate-size (1–2m) ground-based telescopes
- NGC 4151: UV monitoring by a European consortium (led by M.V. Penston and M.-H. Ulrich).
  - Typical sampling interval of 2–3 months.
  - Several major results:
    - close correspondence of UV/optical continuum variations
    - line fluxes correlated with continuum, but different lines respond in different ways (amplitude and time scale)
    - complicated relationship between UV and X-ray
    - variable absorption lines

First Monitoring Programs

- NGC 4151: Lick Observatory by Antonucci and Cohen in 1980-81
  - short time scale response of Balmer lines (<1 month)
  - higher amplitude variability of higher-order Balmer lines and He II λ4686

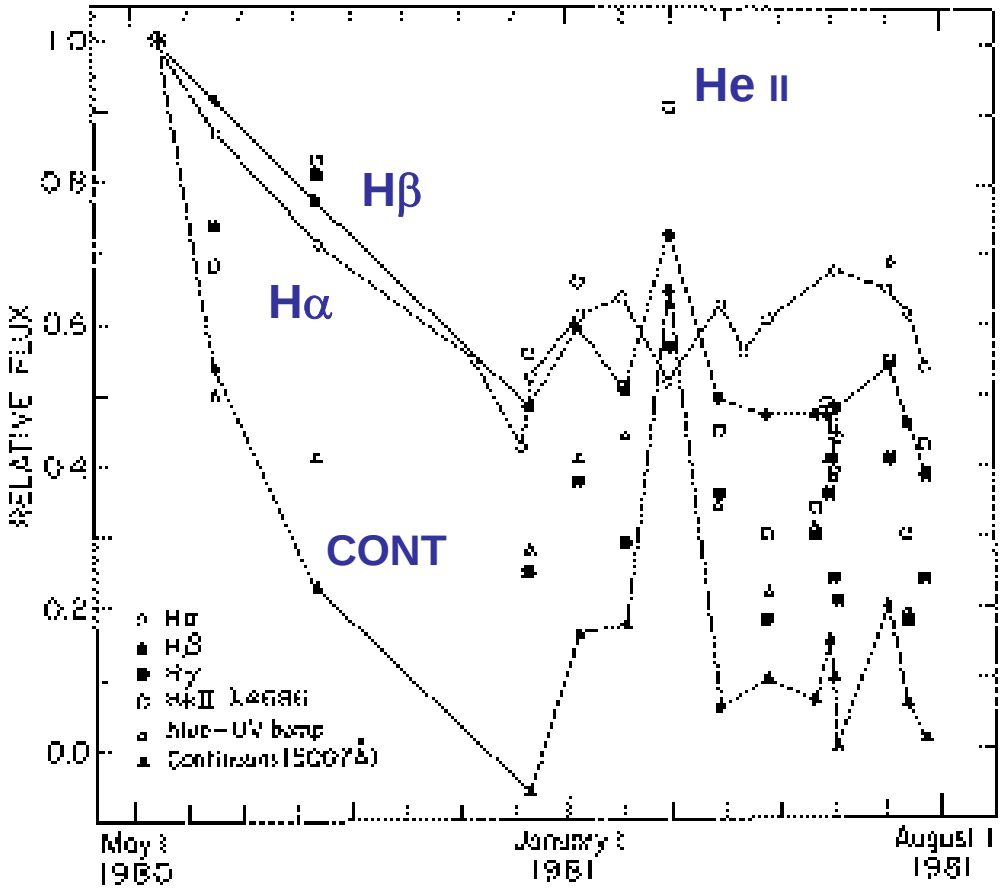

Antonucci & Cohen 1983

First Monitoring Programs

- Akn 120:
  - In optical by Peterson et al. (1983; 1985).
    - Hβ response time suggested BLR less than 1 light month across
    - Suggested serious problem with existing estimates of sizes of broad-line region
  - Higher luminosity source, so monthly sampling provided more critical challenge to BLR models

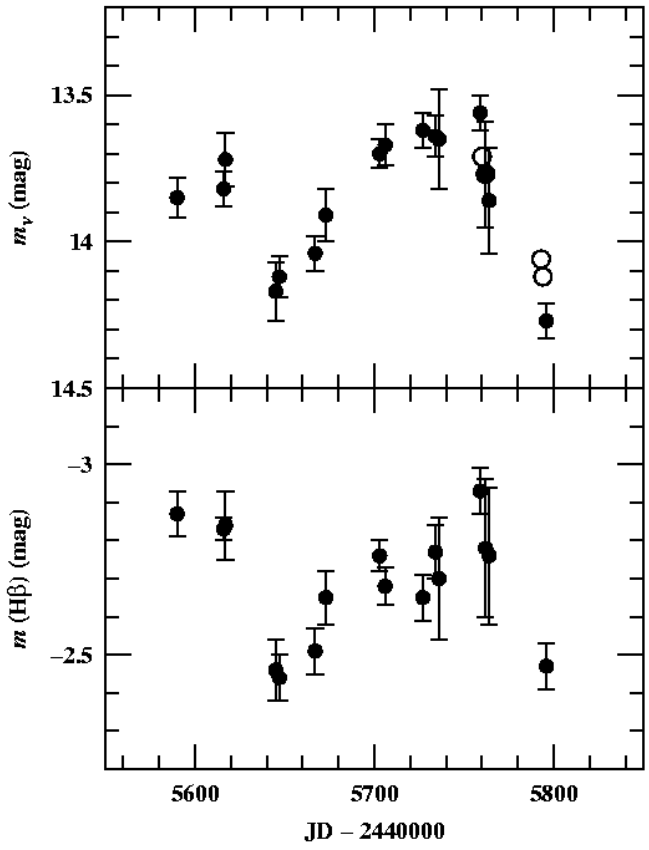

Data from Peterson et al. 1985

Broad-Line Flux and Profile Variability

- Emission-line fluxes vary with the continuum, but with a short time delay.
- Inferences:
  - Gas is photoionized and optically thick
  - Line-emitting region is fairly small

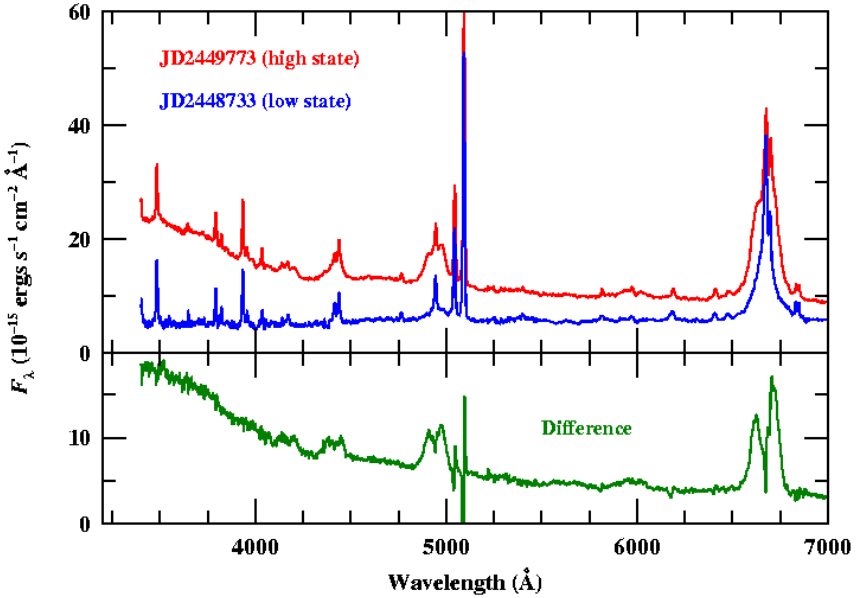

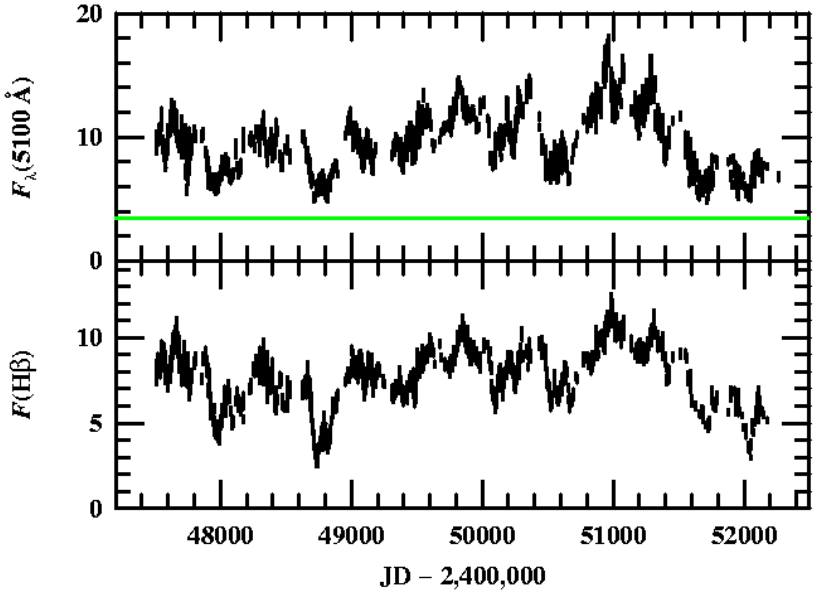

Reverberation Mapping

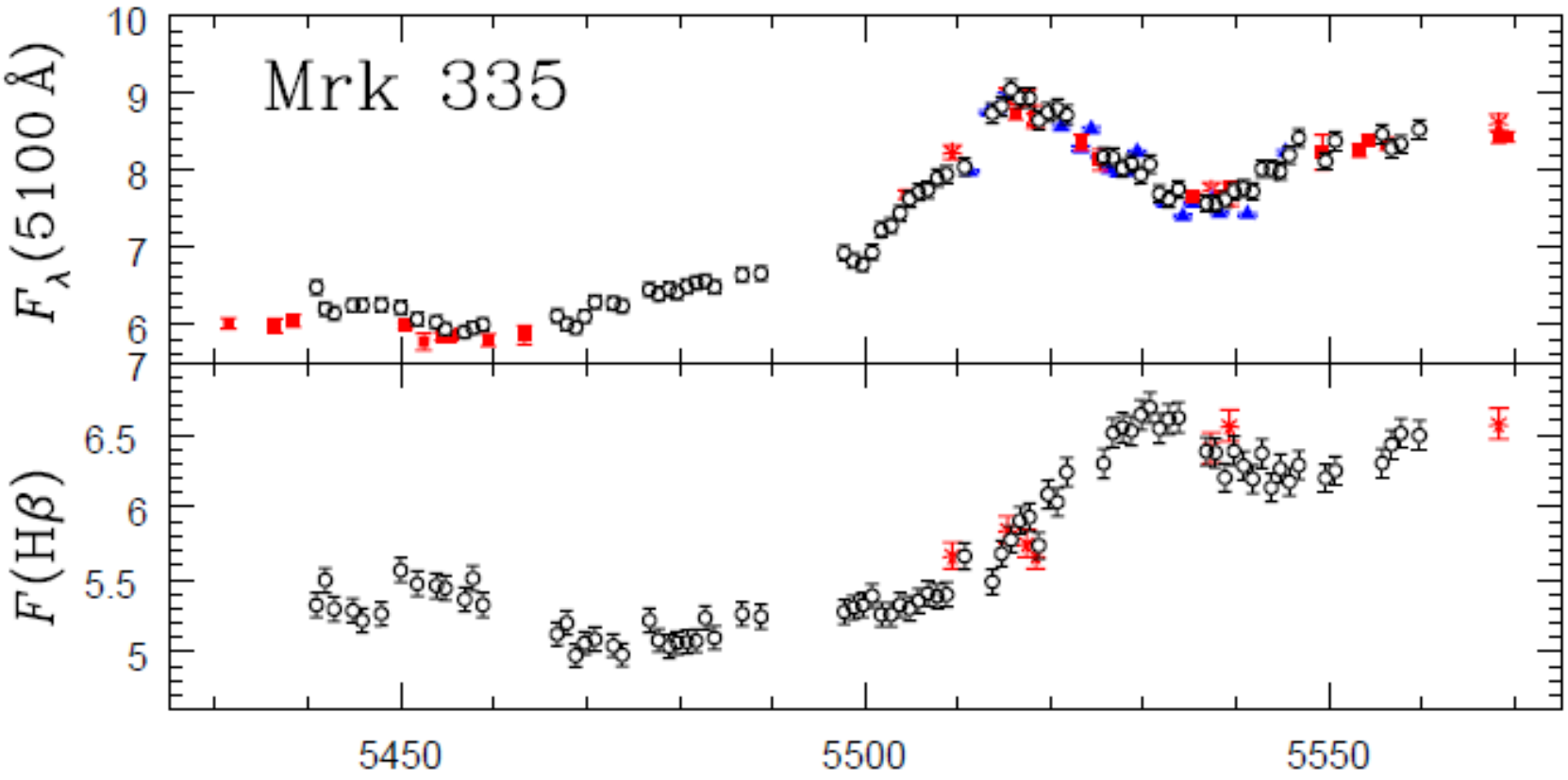

Emission line variations follow those in continuum with a small time delay (14 days here) due to light-travel time across the line emitting region.

Grier+ 2012, ApJ, 744, L4

Reverberation Mapping Assumptions

1) The continuum originates in a point source
2) The most important timescale is the BLR light-crossing time $\tau_{LT} = R/c$.
   - Dynamical time is $\tau_{dyn} = R/\Delta V$, so $\tau_{dyn}/\tau_{LT} = c/\Delta V \approx 100$.
   - Recombination time is $\tau_{rec} \approx (\alpha_B\, n_e)^{-1} \approx 400\ s^{-1}$ for a density of $10^{10}\ cm^{-3}$.
3) There is a simple, though not necessarily linear, relationship between the observable UV/optical continuum and the ionizing continuum

Reverberation Mapping Concepts: Response of an Edge-On Ring

- Suppose line-emitting clouds are on a circular orbit around the central source.
- Compared to the signal from the central source, the signal from anywhere on the ring is delayed by light-travel time.
- Time delay at position (r,θ) is $\tau = (1 + \cos\theta) r / c$

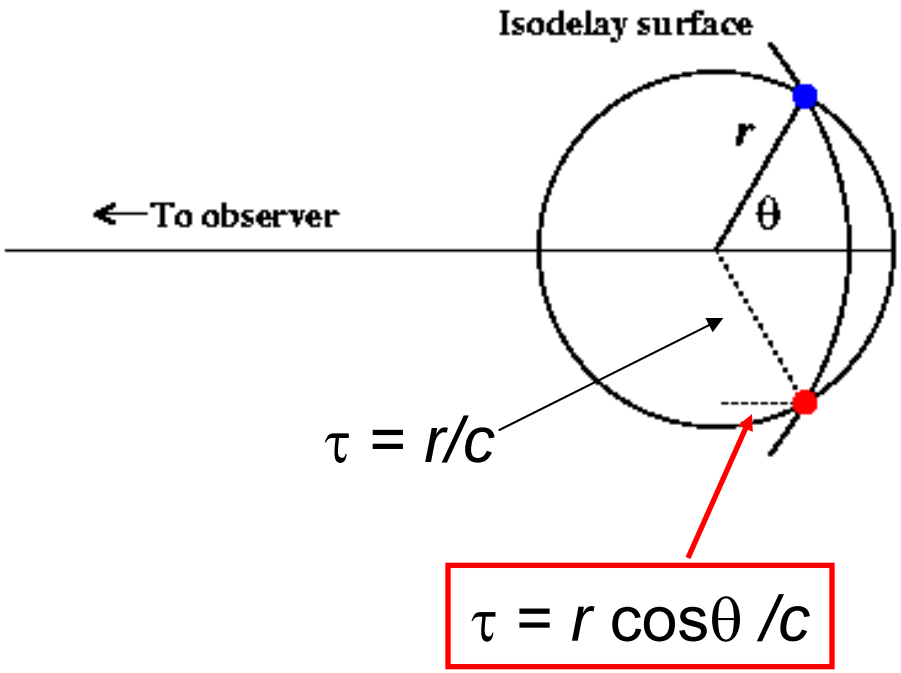

The isodelay surface is a parabola:

$$r = \frac{c\tau}{1 + \cos\theta}$$

“Isodelay Surfaces”

All points on an “isodelay surface” have the same extra light-travel time to the observer, relative to photons from the continuum source.

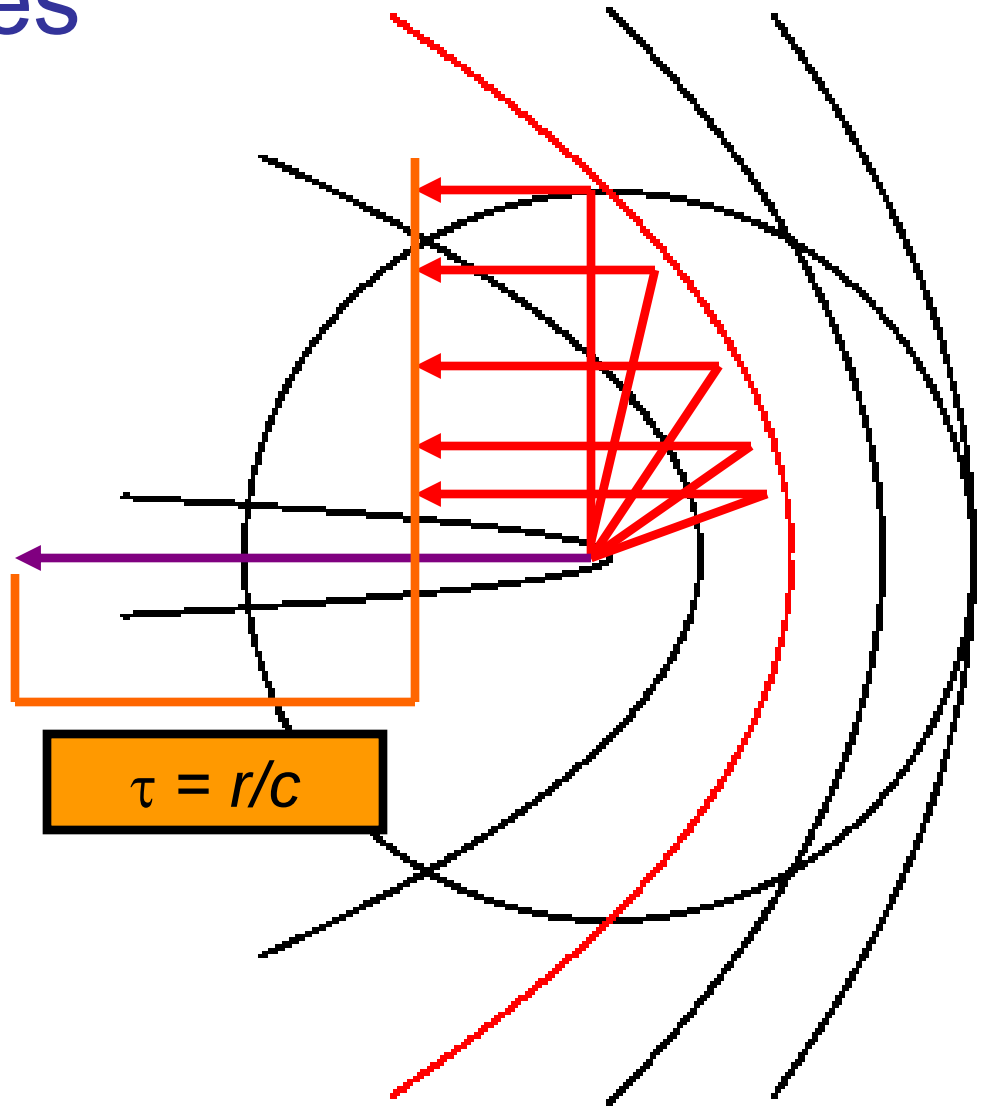

Velocity-Delay Map for an Edge-On Ring

- Clouds at intersection of isodelay surface and orbit have line-of-sight velocities $V = \pm V_{orb} \sin \theta$.
- Response time is $\tau = (1 + \cos \theta) r/c$
- Circular orbit projects to an ellipse in the (V, τ) plane.

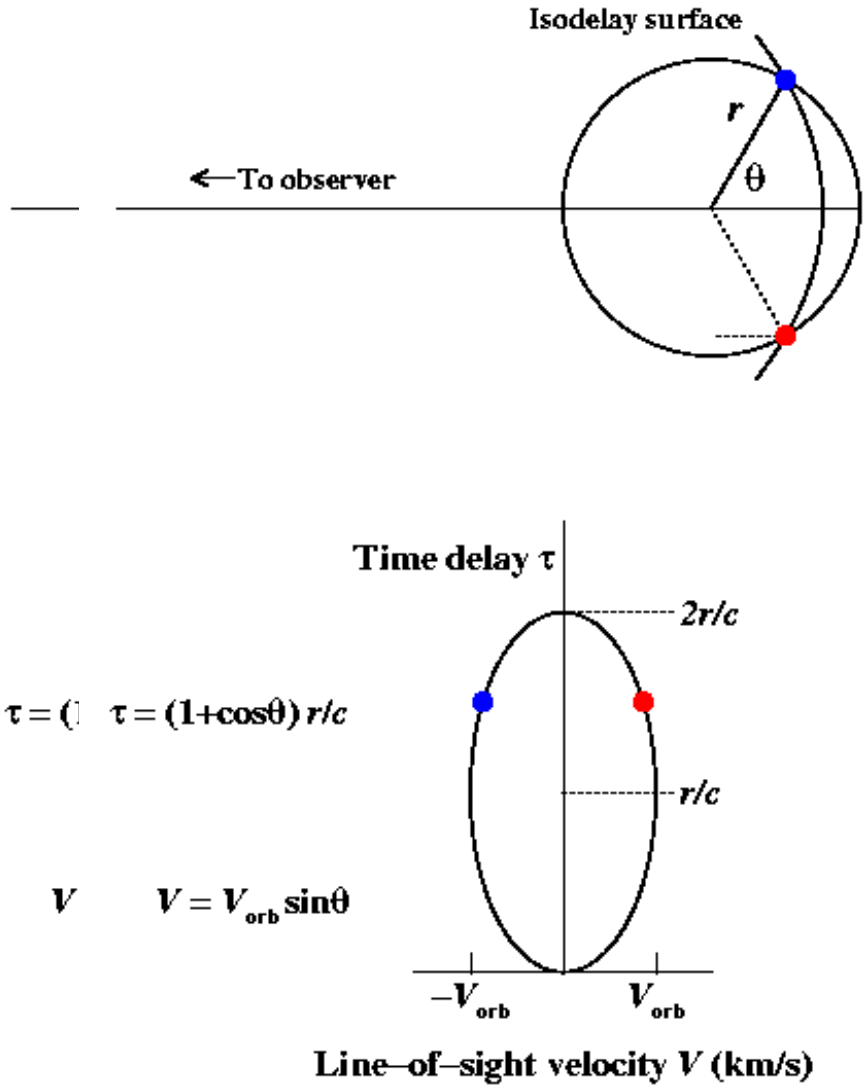

Velocity-Delay Map

Configuration space

Velocity-delay space

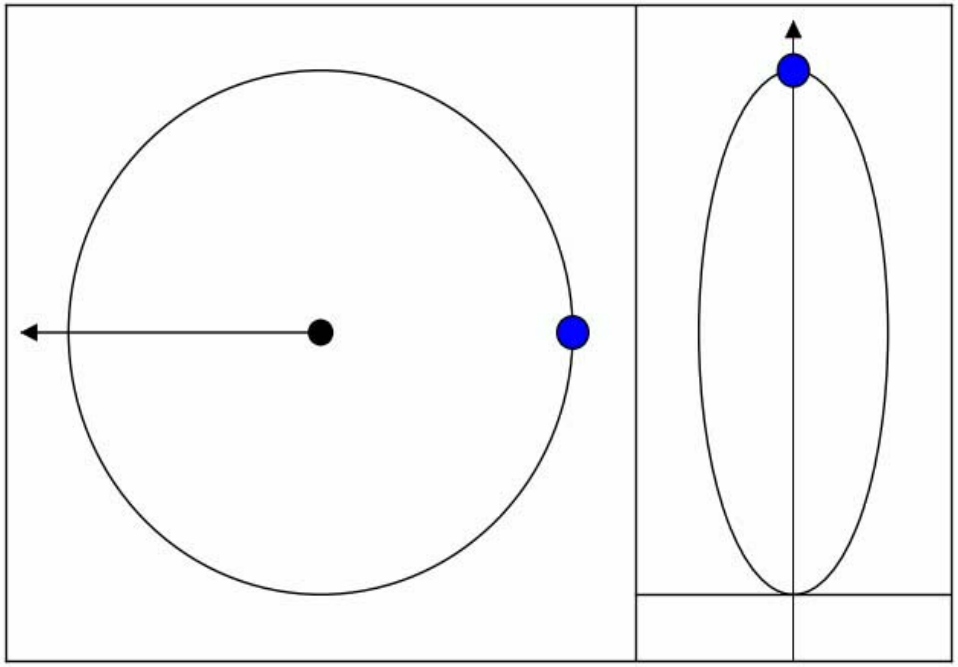

To observer

Time delay

Doppler velocity

Projection in Time Delay

Assume isotropy

$$\Psi(\theta) = \varepsilon$$

Transform to time-delay (observable)

$$\Psi(\tau)\, d\tau = \Psi(\theta) \frac{d\theta}{d\tau}\, d\tau$$

$$\tau = (1 + \cos\theta) R / c$$

$$\frac{d\tau}{d\theta} = -\frac{R}{c} \sin\theta$$

Do some algebra

$$\Psi(\tau)\, d\tau = \frac{\varepsilon}{R(2c\tau / R)^{1/2} (1 - c\tau / 2R)^{1/2}}\, d\tau$$

Delay Map for a Ring

Symmetry, or some calculus, will show that:

$$\langle \tau \rangle = \frac{\int_0^\infty \tau \, \Psi(\tau) \, d\tau}{\int_0^\infty \Psi(\tau) \, d\tau} = \frac{R}{c}$$

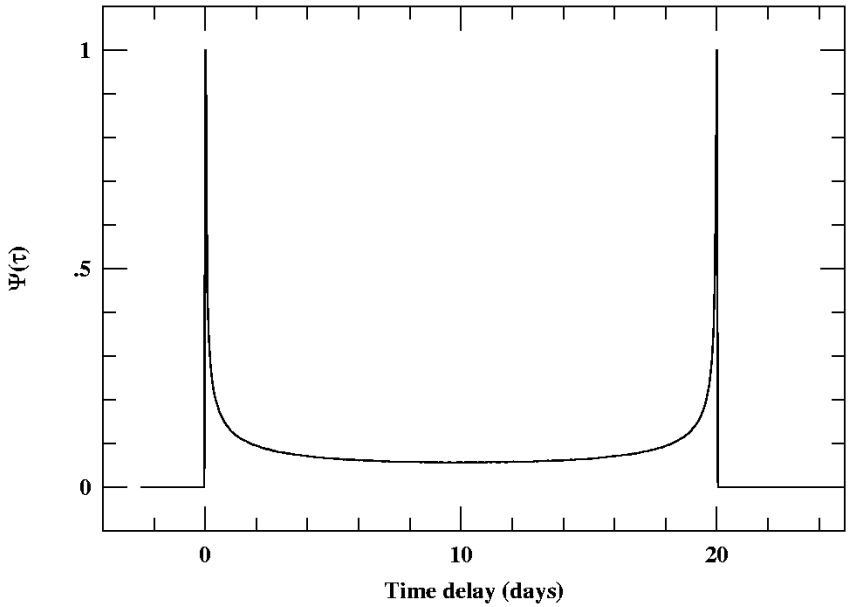

Projection in Line-of-Sight Velocity

Assume isotropy

$$\Psi(\theta) = \varepsilon$$

Transform to LOS velocity (observable)

$$\Psi(V_{\rm LOS})\, dV_{\rm LOS} = \Psi(\theta) \frac{d\theta}{dV_{\rm LOS}}\, dV_{\rm LOS}$$

$$V_{\rm LOS} = -V_{\rm orb} \sin\theta$$

$$\frac{dV_{\rm LOS}}{d\theta} = -V_{\rm orb} \cos\theta$$

Do some algebra again

$$\Psi(V_{\rm LOS})\, dV_{\rm LOS} = \frac{\varepsilon}{V_{\rm orb}(1-(V_{\rm LOS}/V_{\rm orb})^2)^{1/2}}\, dV_{\rm LOS}$$

Line Profile for a Ring

- Characterize line width
  - FWHM = $2V_{orb}$
  - σ_{line}

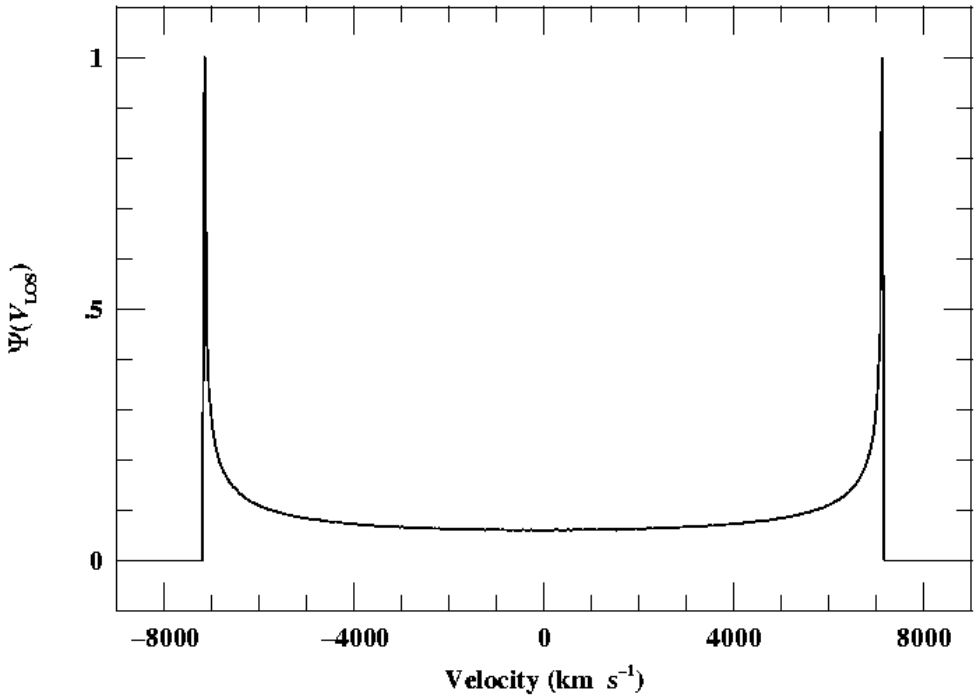

$$\sigma_{\rm line} = \left(\left\langle V_{\rm LOS}^2 \right\rangle - \left\langle V_{\rm LOS} \right\rangle^2 \right)^{1/2} = \left[\frac{\int_{-V_{\rm orb}}^{V_{\rm orb}} V_{\rm LOS}^2 \Psi(V_{\rm LOS})\, dV_{\rm LOS}}{\int_{-V_{\rm orb}}^{V_{\rm orb}} \Psi(V_{\rm LOS})\, dV_{\rm LOS}} - \left(\frac{\int_{-V_{\rm orb}}^{V_{\rm orb}} V_{\rm LOS} \Psi(V_{\rm LOS})\, dV_{\rm LOS}}{\int_{-V_{\rm orb}}^{V_{\rm orb}} \Psi(V_{\rm LOS})\, dV_{\rm LOS}} \right)^2 \right]^{1/2} = \left(\frac{V_{\rm LOS}^2}{2} \right)^{1/2}$$

For a ring, FWHM/σ_{line} = $2 \times 2^{1/2}$ = 2.83

Thick Geometries

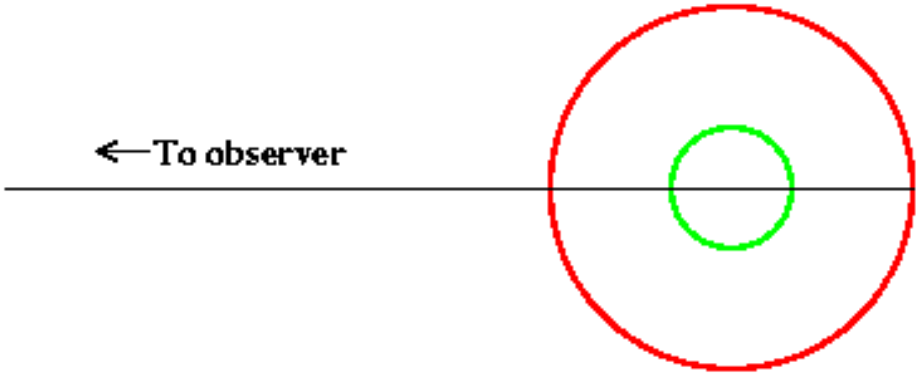

- Generalization to a disk or thick shell is trivial.
- General result is illustrated with simple two ring system.

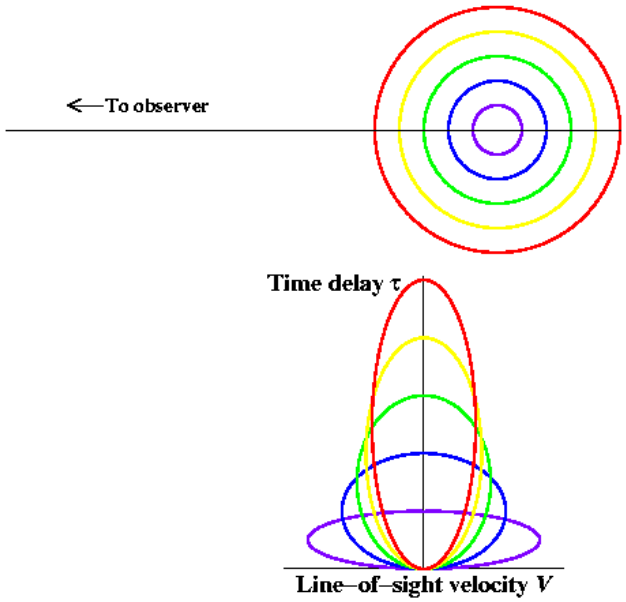

A multiple-ring system

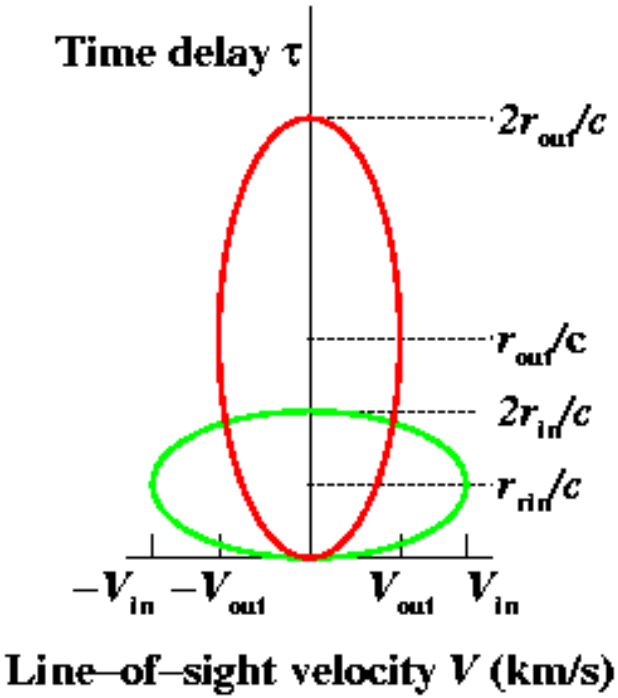

Time after continuum outburst

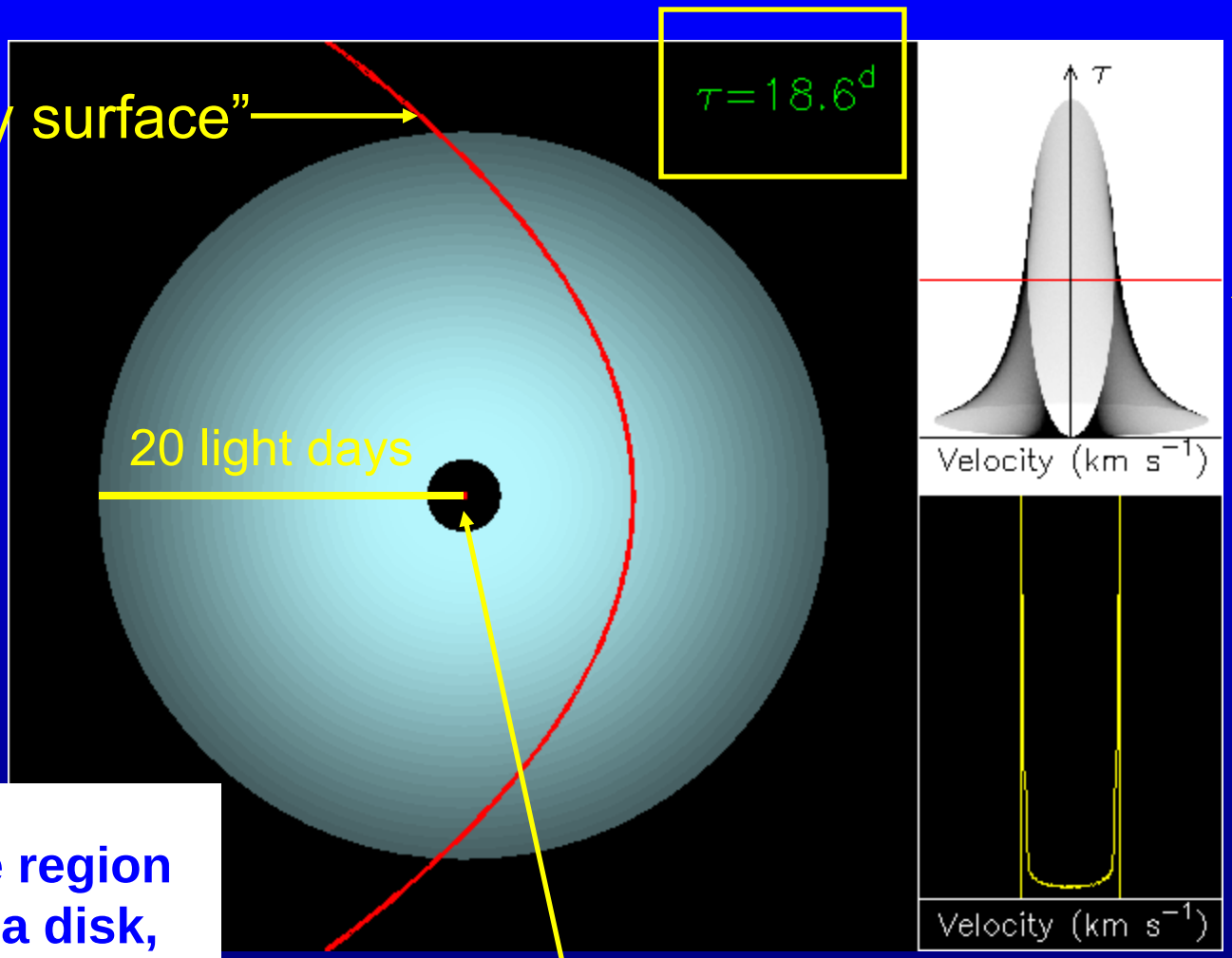

Time delay

Broad-line region as a disk, 2–20 light days

Black hole/accretion disk

Line profile at current time delay

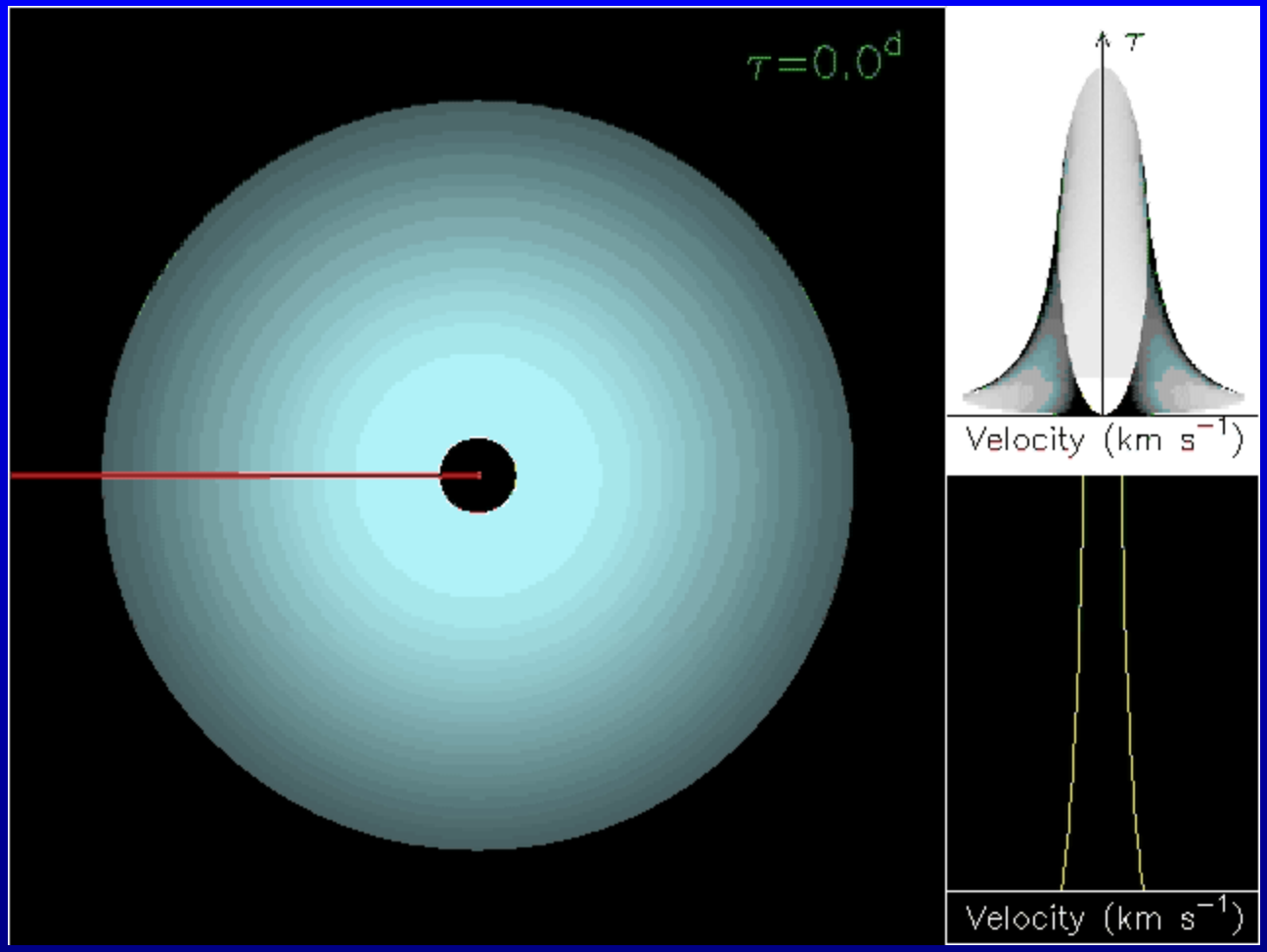
τ=0.0d
τ
Velocity (km s−1)
Velocity (km s−1)

Reverberation Response of an Emission Line to a Variable Continuum

The relationship between the continuum and emission can be taken to be:

$$L(V,t) = \int \Psi(V,\tau)\, C(t-\tau)\, d\tau$$

Velocity-resolved emission-line light curve

"Velocity-delay map"

Continuum light curve

Velocity-delay map is observed line response to a δ-function outburst

Required time sampling, duration, and *S/N* makes velocity-delay map recovery very difficult.

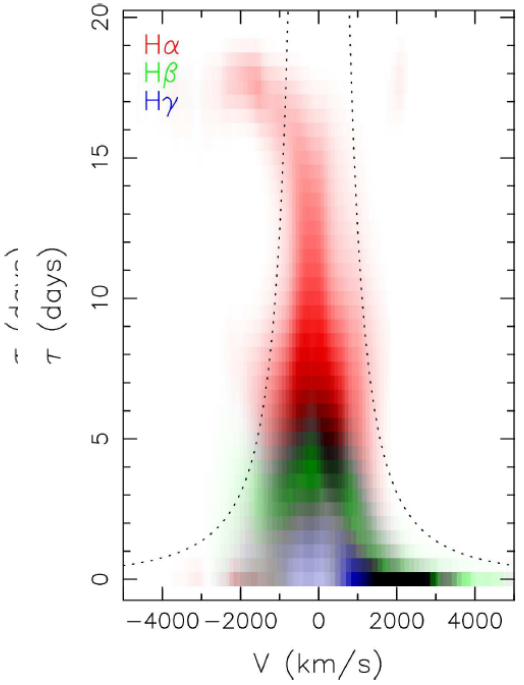

Arp 151

LAMP: Bentz+ 2010

A Complex Multicomponent Broad-Line Region?

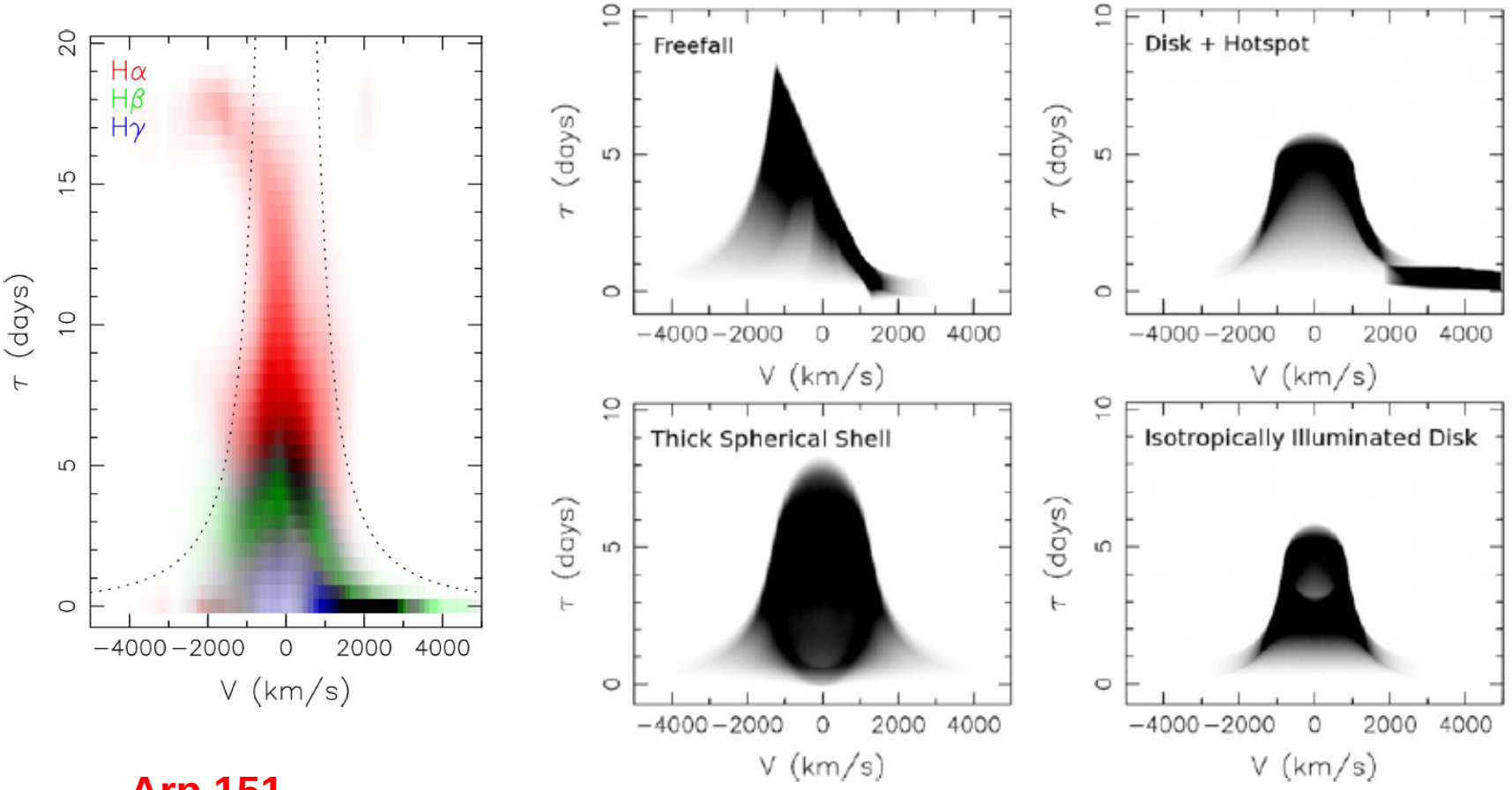

Arp 151
LAMP: Bentz+ 2010

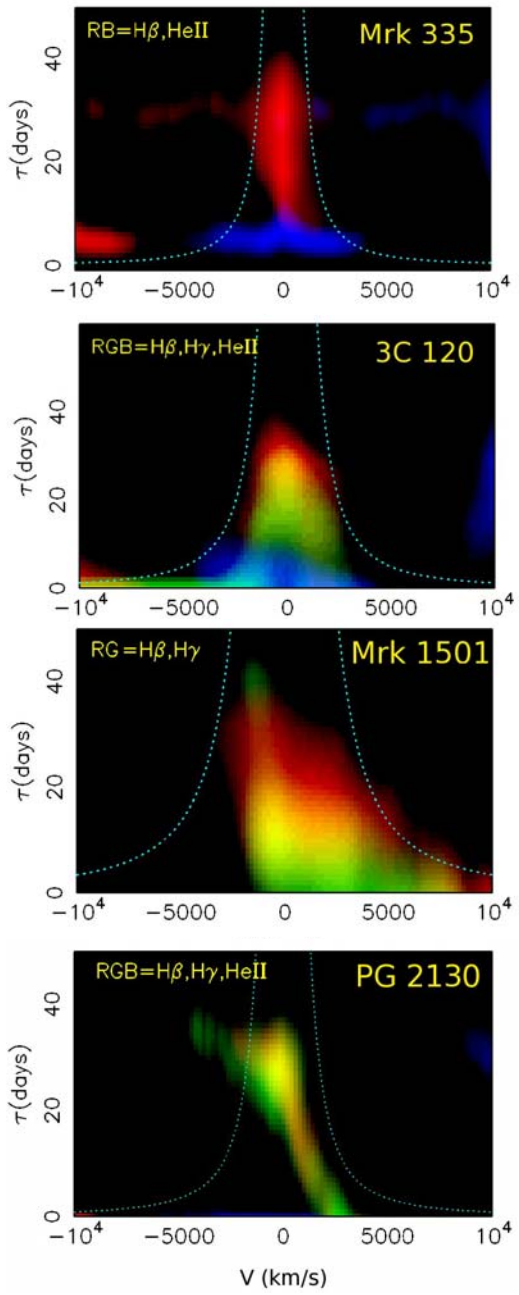

Toy Models

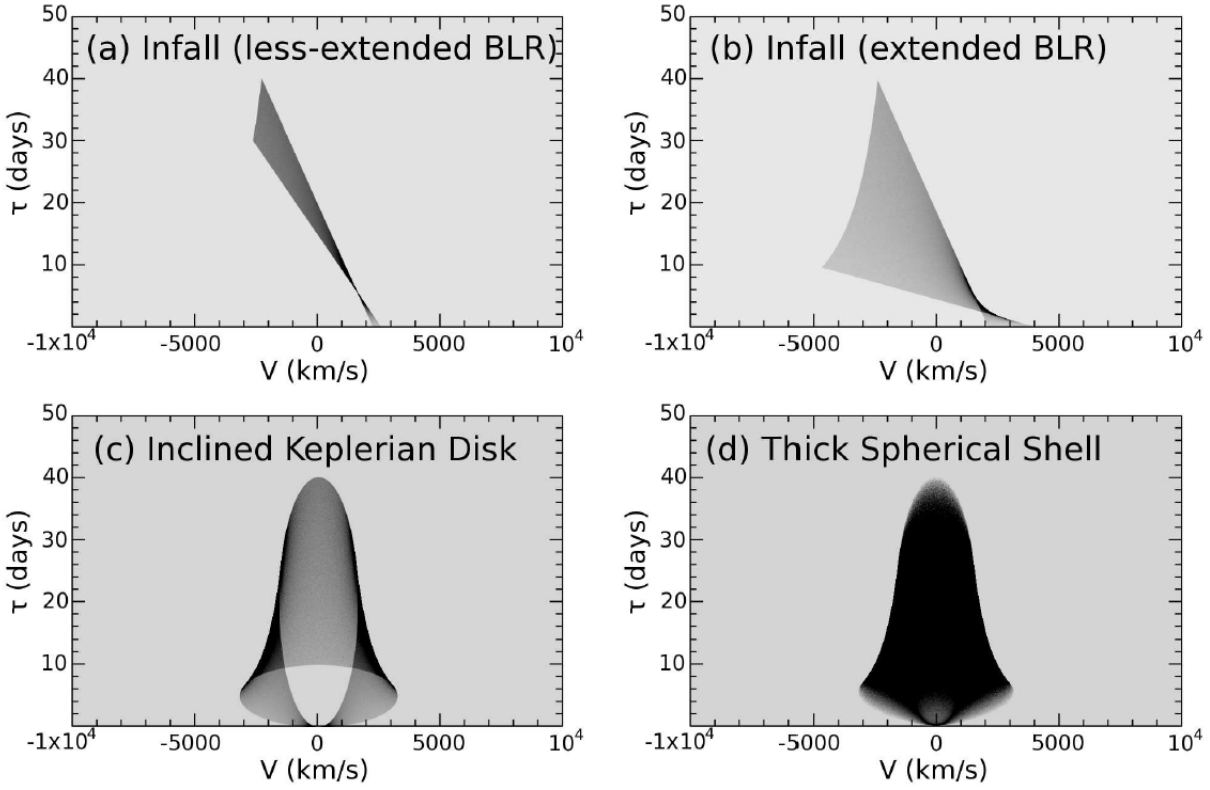

Grier+ 2013, ApJ, 764:47

Emission-Line Lags

- Because the data requirements are *relatively* modest, it is most common to determine the cross-correlation function and obtain the "lag" (mean response time):

$$\mathrm{CCF}(\tau) = \int \Psi(\tau')\ \mathrm{ACF}(\tau - \tau')\, d\tau'$$

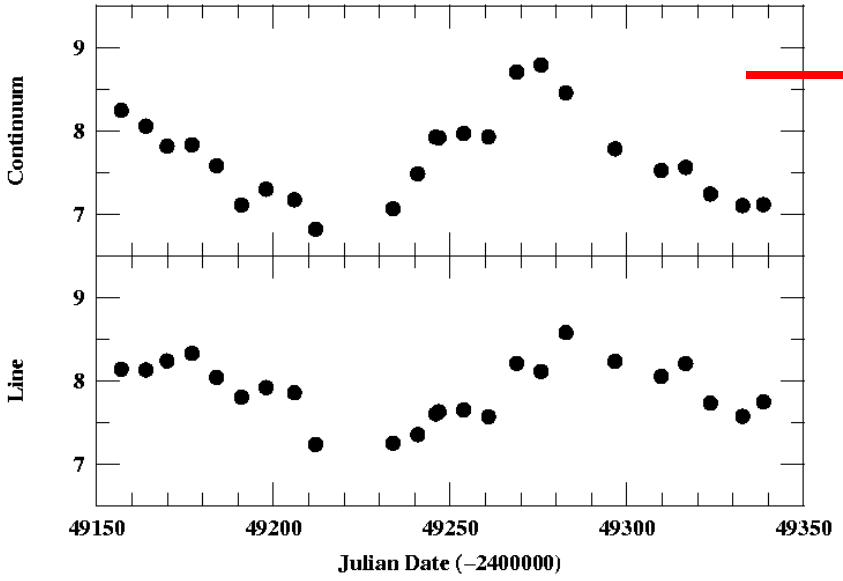

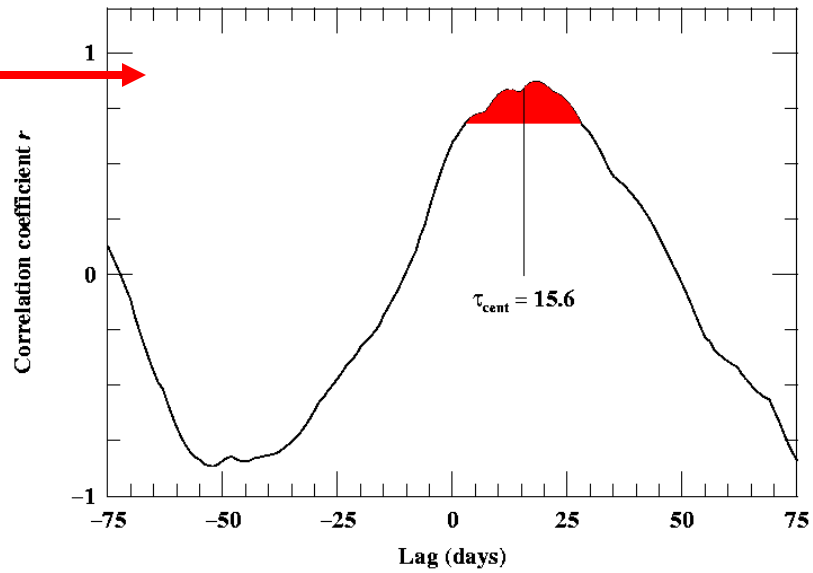

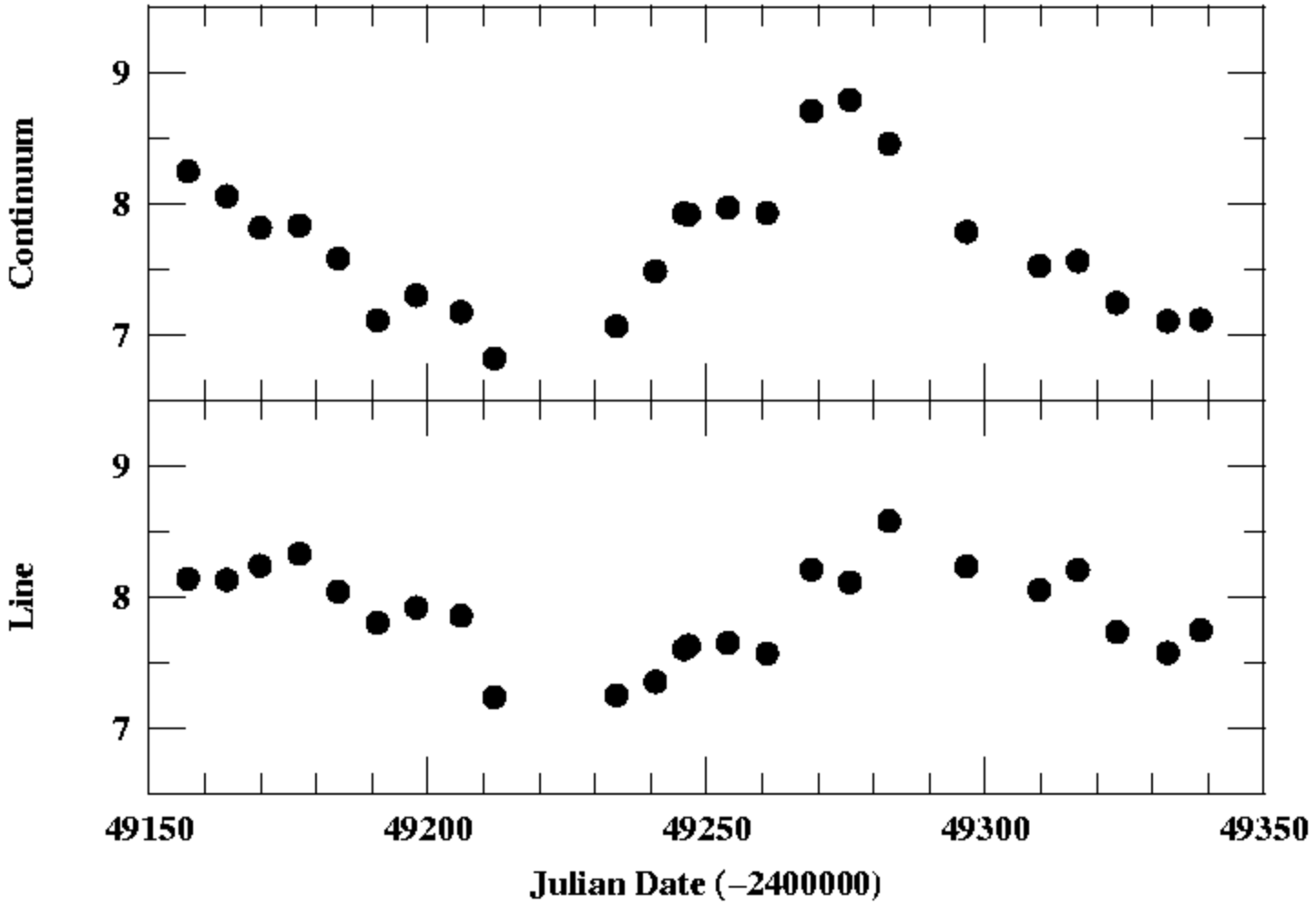

Determine the shift or “lag” between these two series that maximizes the linear correlation coefficient.
Data on Mrk 335.

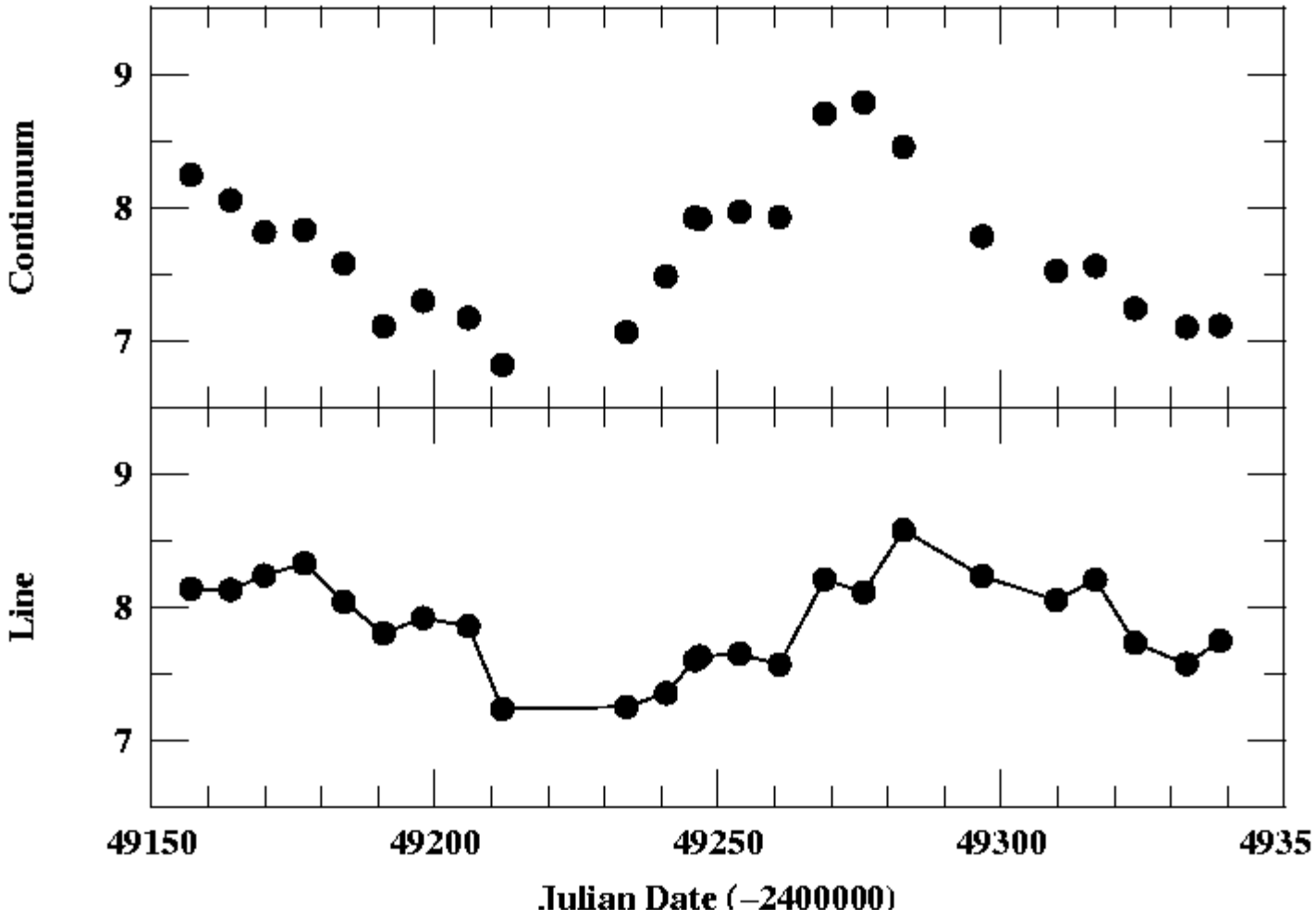

Practical problem: in general, data are not evenly spaced. One solution is to interpolate between real data points.

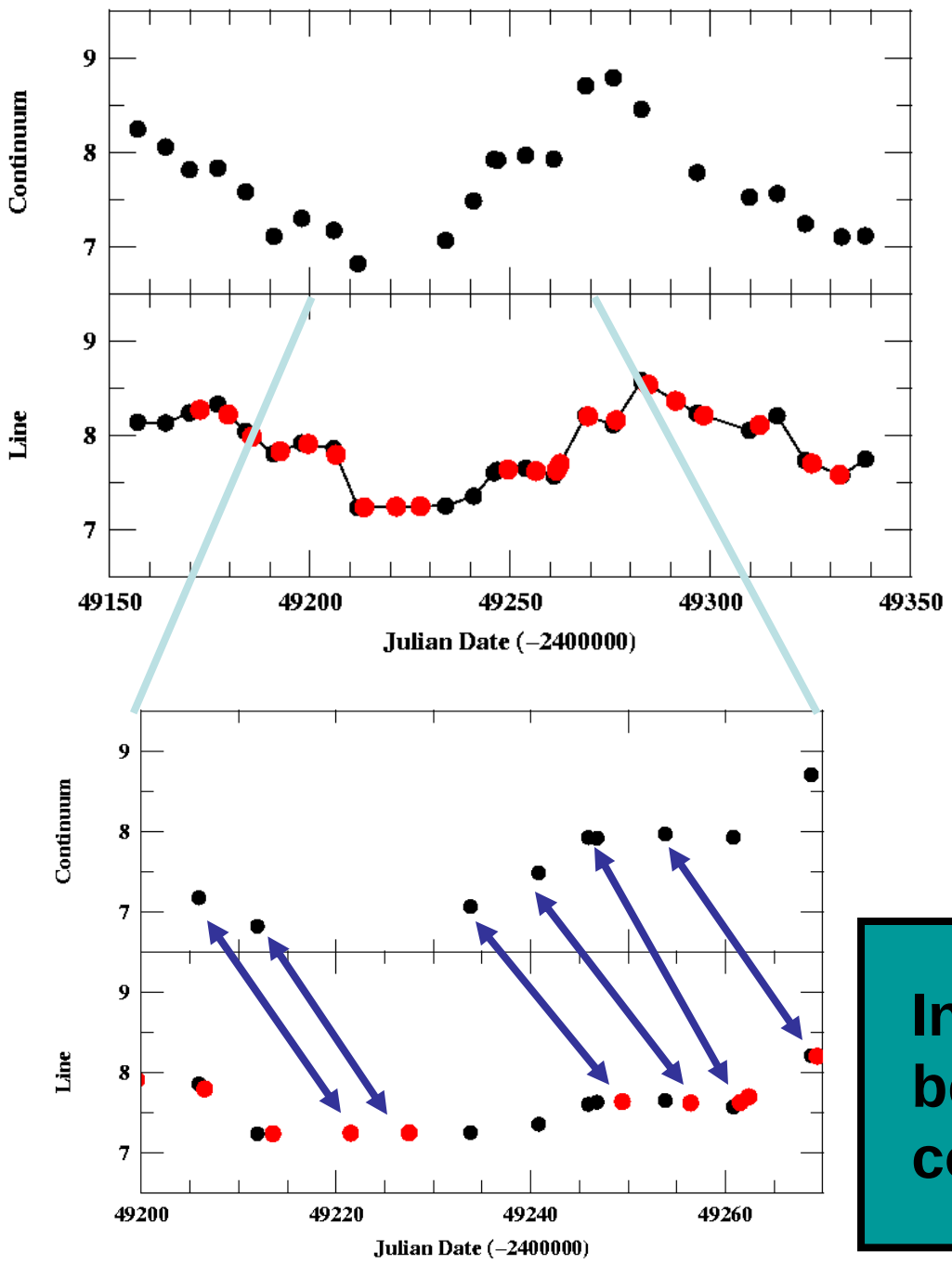

Each real datum $C(t)$ in one time series is matched with an interpolated value $L(t + \tau)$ in the other time series and the linear correlation coefficient is computed for all possible values of the lag τ.

Interpolated line points lag behind corresponding continuum points by 16 days.

Uncertainties in Cross-Correlation Lags

- Commonly used method is a model-independent Monte-Carlo method called "FR/RSS":
  - FR: Flux redistribution
    - accounts for the effects of uncertainties in flux measurement
  - RSS: Random subset selection
    - accounts for effects of sampling in time

Bootstrap Method

- RSS is based on a computationally intensive method for evaluating significance of linear correlation known as the "bootstrap method".
- Bootstrap method:
  - for *N* real data points, select at random *N* points without regard to whether or not they have been previously selected.
  - Determine *r* for this subset
  - Repeat many times to obtain a distribution in the value of *r*. From this distribution, compute the mean and standard deviation for *r*.

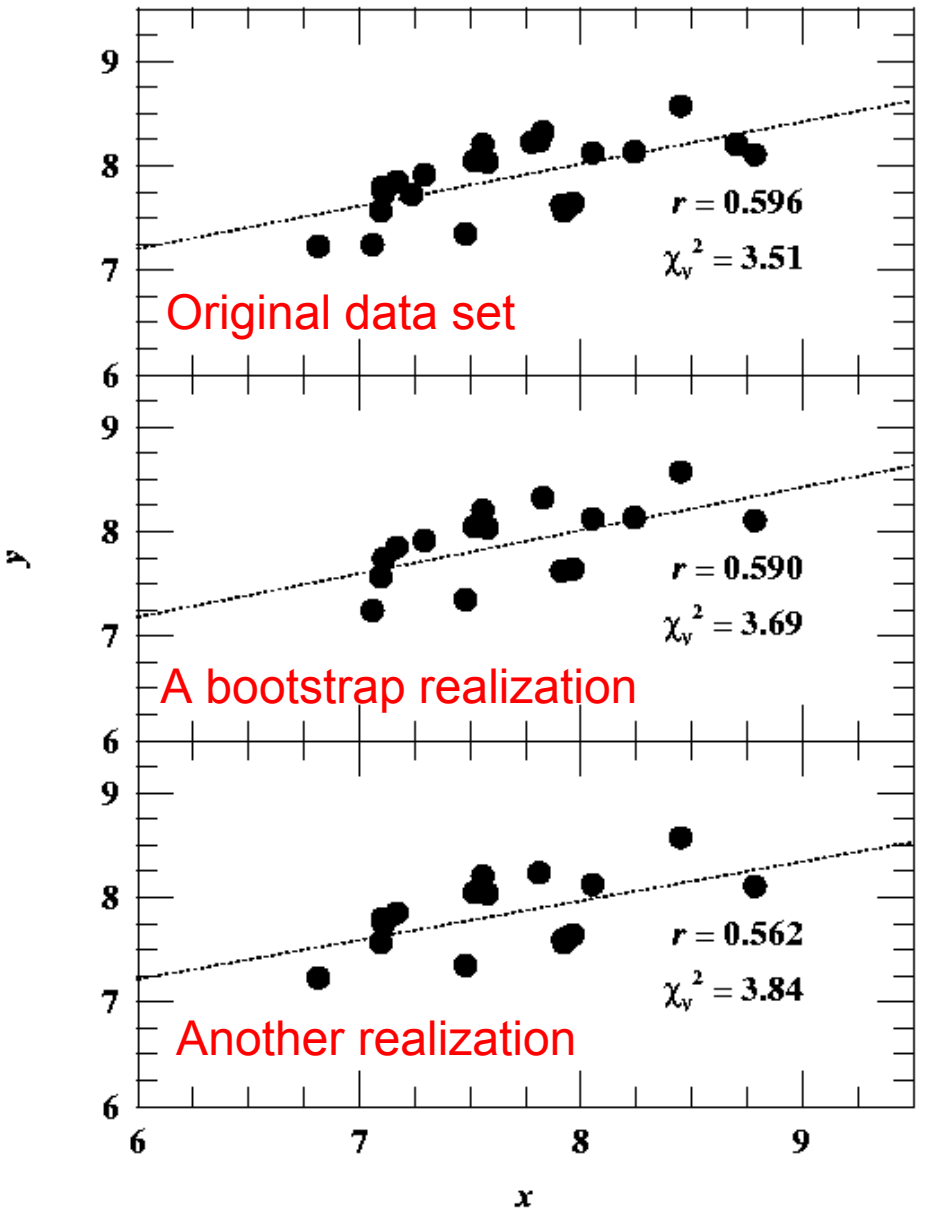

Random Subset Selection

- How do you deal with redundant selections in a time series, where order matters? Either:
  - Ignore redundant selections
    - Each realization has typically 1/*e* fewer points than the original (origin of the name RSS).
    - Numerical experiments show that this then gives a conservative error on the lag (the real uncertainty may be somewhat smaller).
  - Weight each datum according to number of times selected
    - Philosophically closer to original bootstrap.

Flux Redistribution

- Assume that flux uncertainties are Gaussian distributed about measured value, with uncertainty σ.
- Take each measured flux value and alter it by a random Gaussian deviate.
- Decrease σ by factor $n^{1/2}$, where n is the number of times the point is selected.

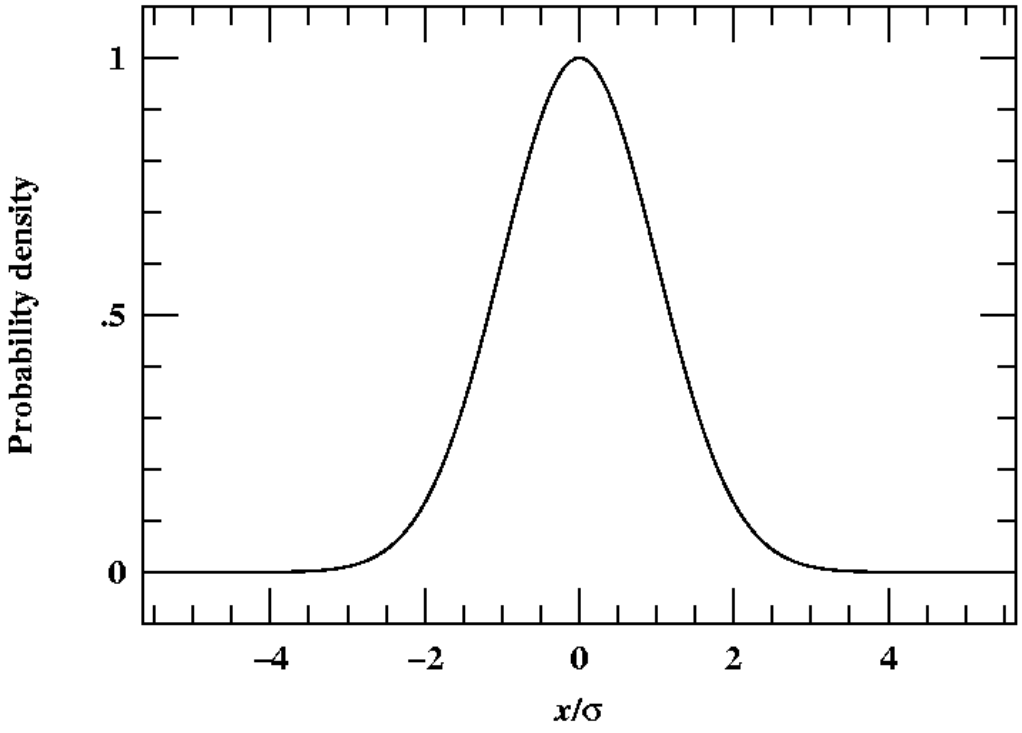

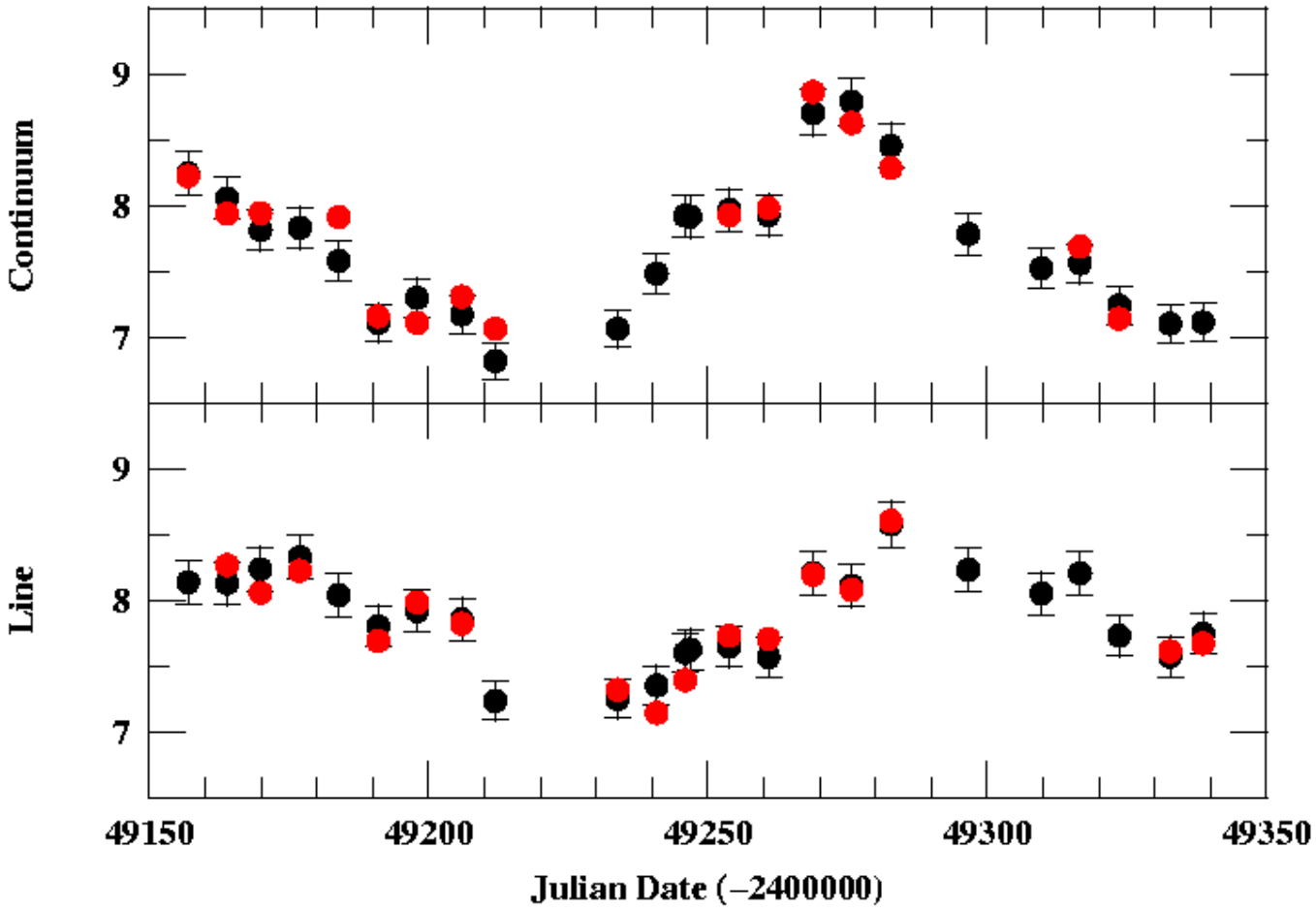

A single FR/RSS realization. Red points are selected at random from among the real (black) points, redundant points are discarded, and surviving points redistributed in flux using random Gaussian deviates scaled by the quoted uncertainty for each point. The realization shown here gives τ_{cent} = 17.9 days (value for original data is 15.6 days)

Cross-Correlation Centroid Distribution

- Many FR/RSS realizations are used to build up the "cross-correlation centroid distribution" (CCCD).
- The rms width of this distribution (which can be non-Gaussian) can be used as an estimate of the lag.

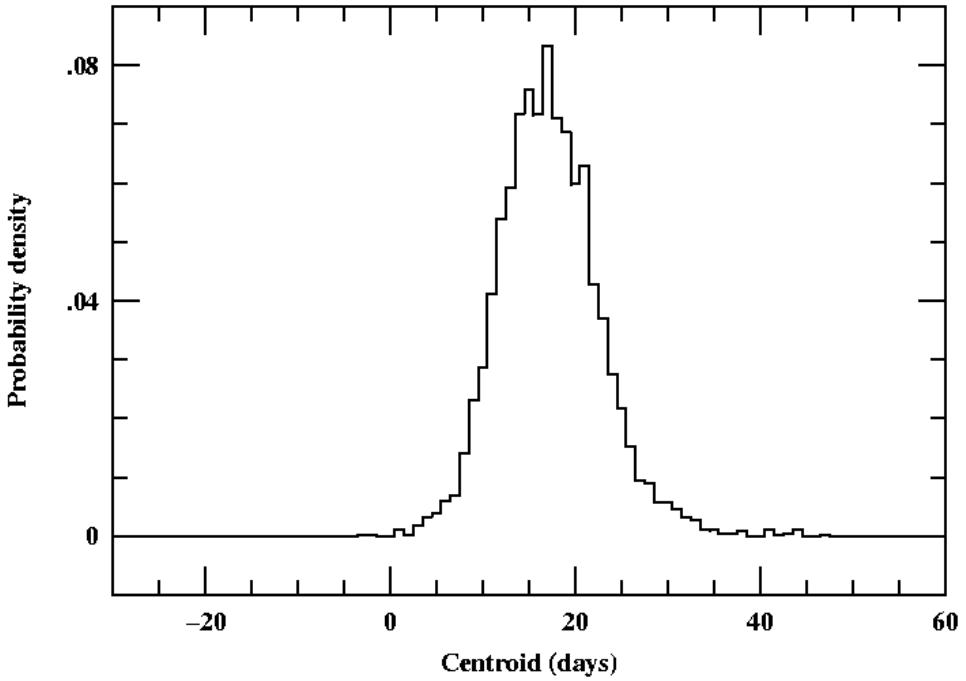

Mrk 335 FR/RSS result:

$$\tau_{\rm cent} = 15.6^{+7.2}_{-3.1}\ {\rm days}$$

A New Reverberation Methodology

- Continuum light curves well described by damped random walk (DRW).
- To characterize DRW:
  - Amplitude
  - Damping time scale
  - Both depend on luminosity
  - Model all possible continuum behaviors in gaps
- A likelihood estimator can be used to identify the most probable lags.
  - Based on statistical process modeling by Press, Rybicki, & Hewitt (1992), Rybicki & Press (1992), and Rybicki & Kleyna (1994).

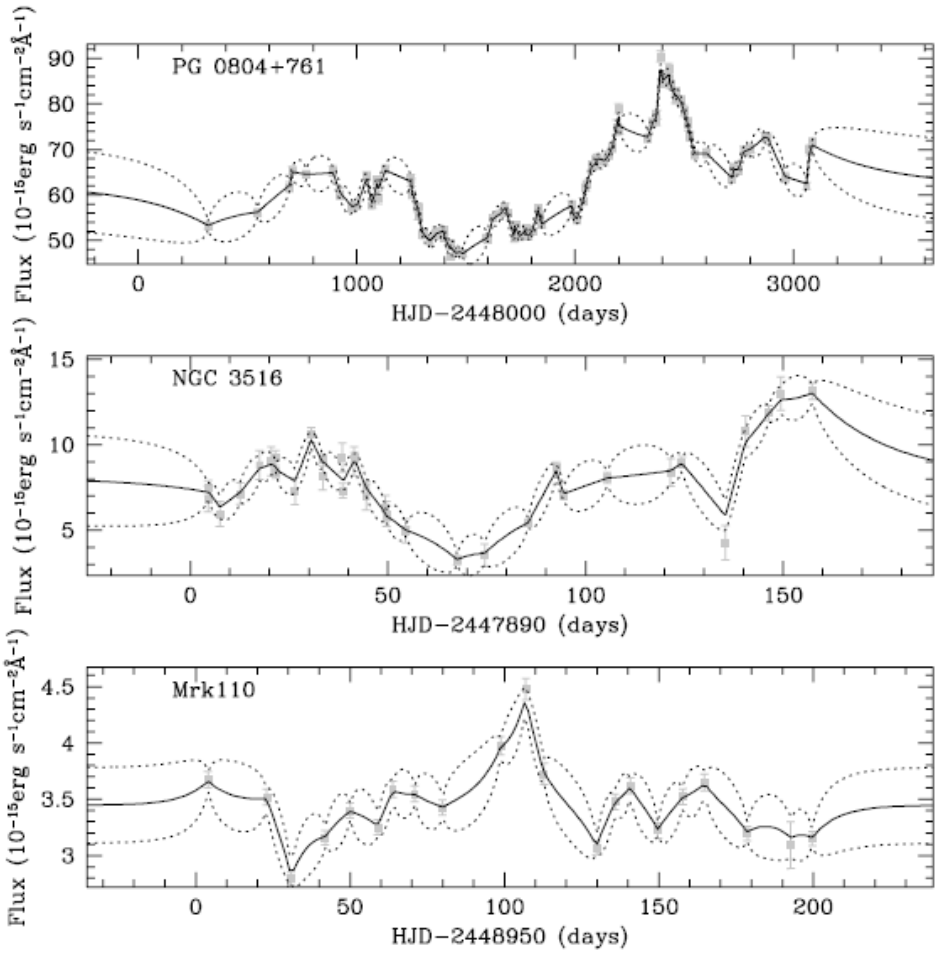

Ohio State implementation: *JAVELIN*
Zu, Kochanek, & Peterson 2011

A New Reverberation Methodology

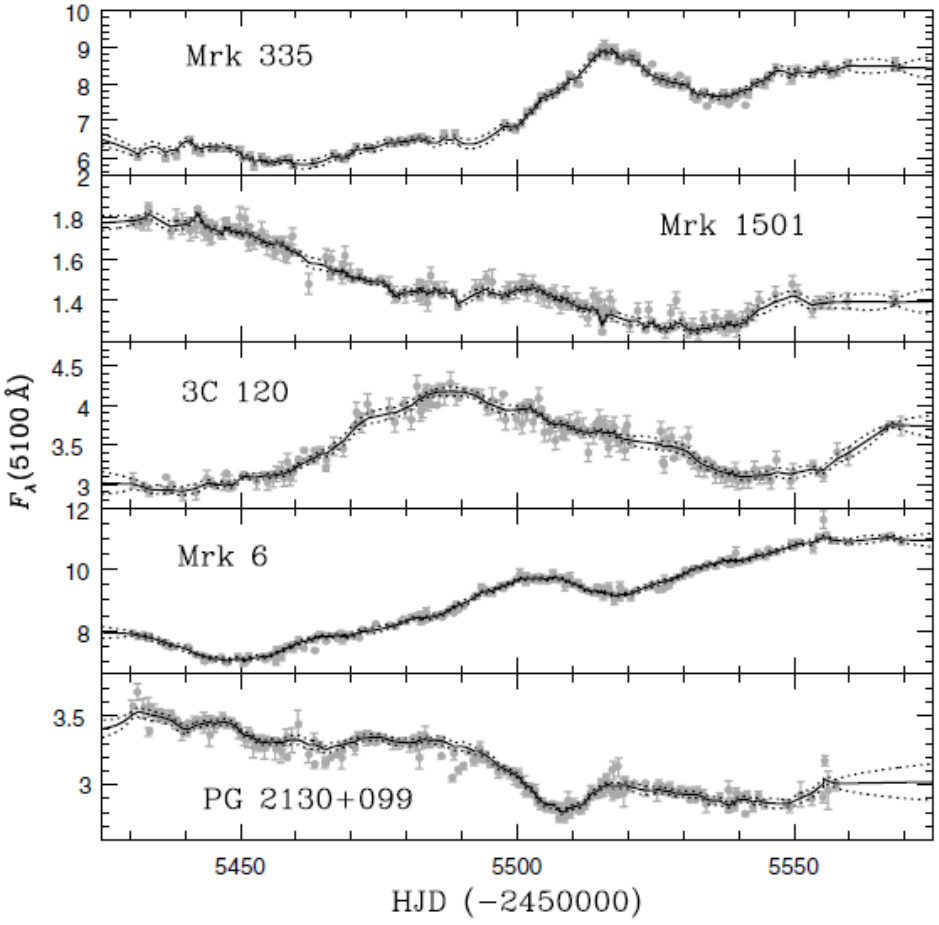

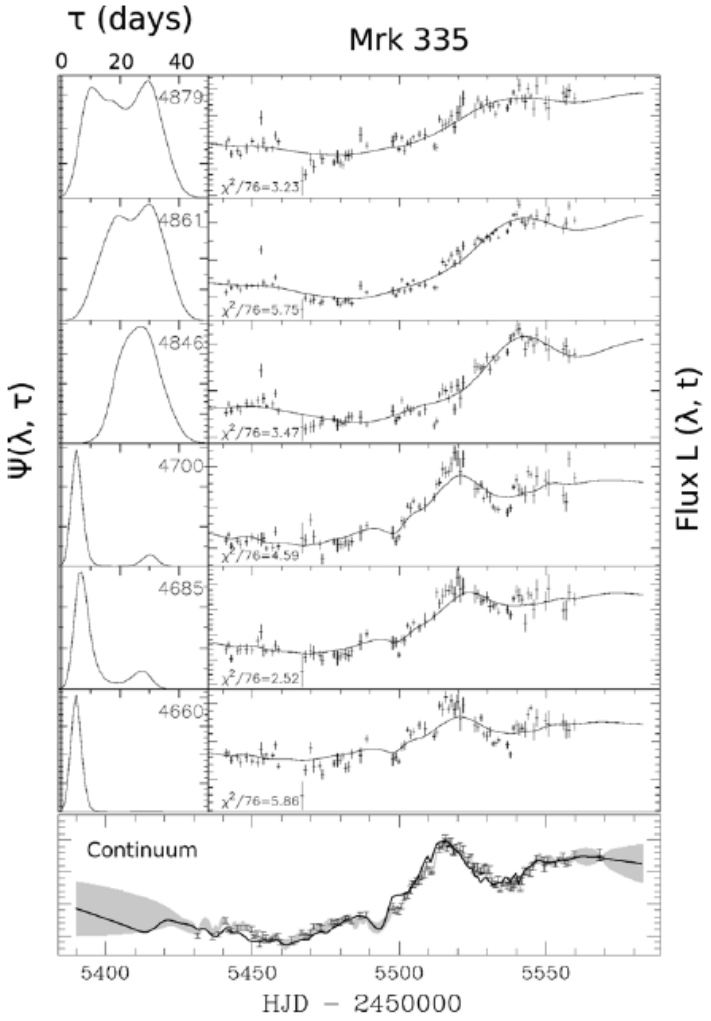

Grier+ 2013, ApJ, 764:47

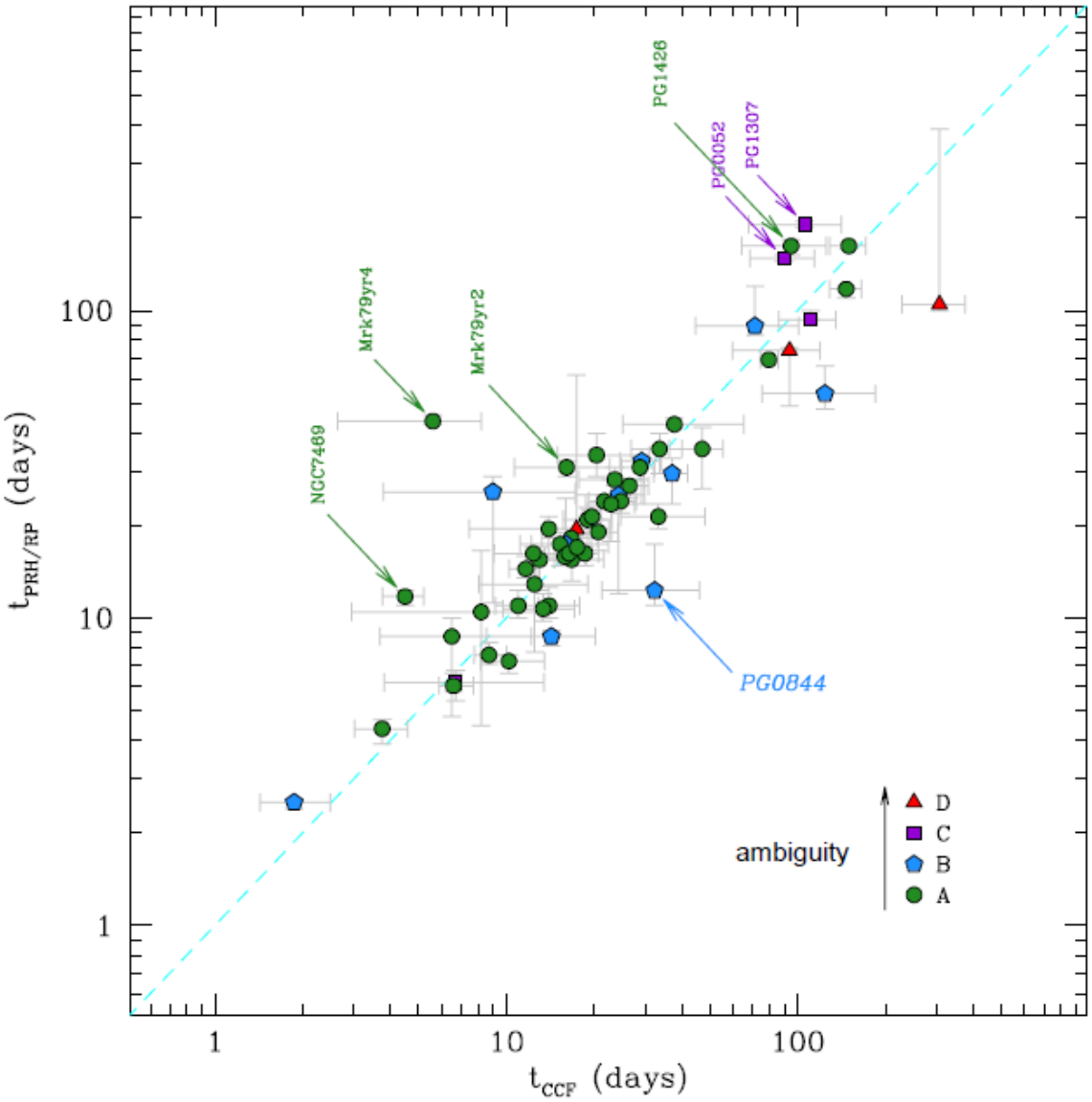

Results are in good agreement with results from CCF and formal errors are somewhat smaller.

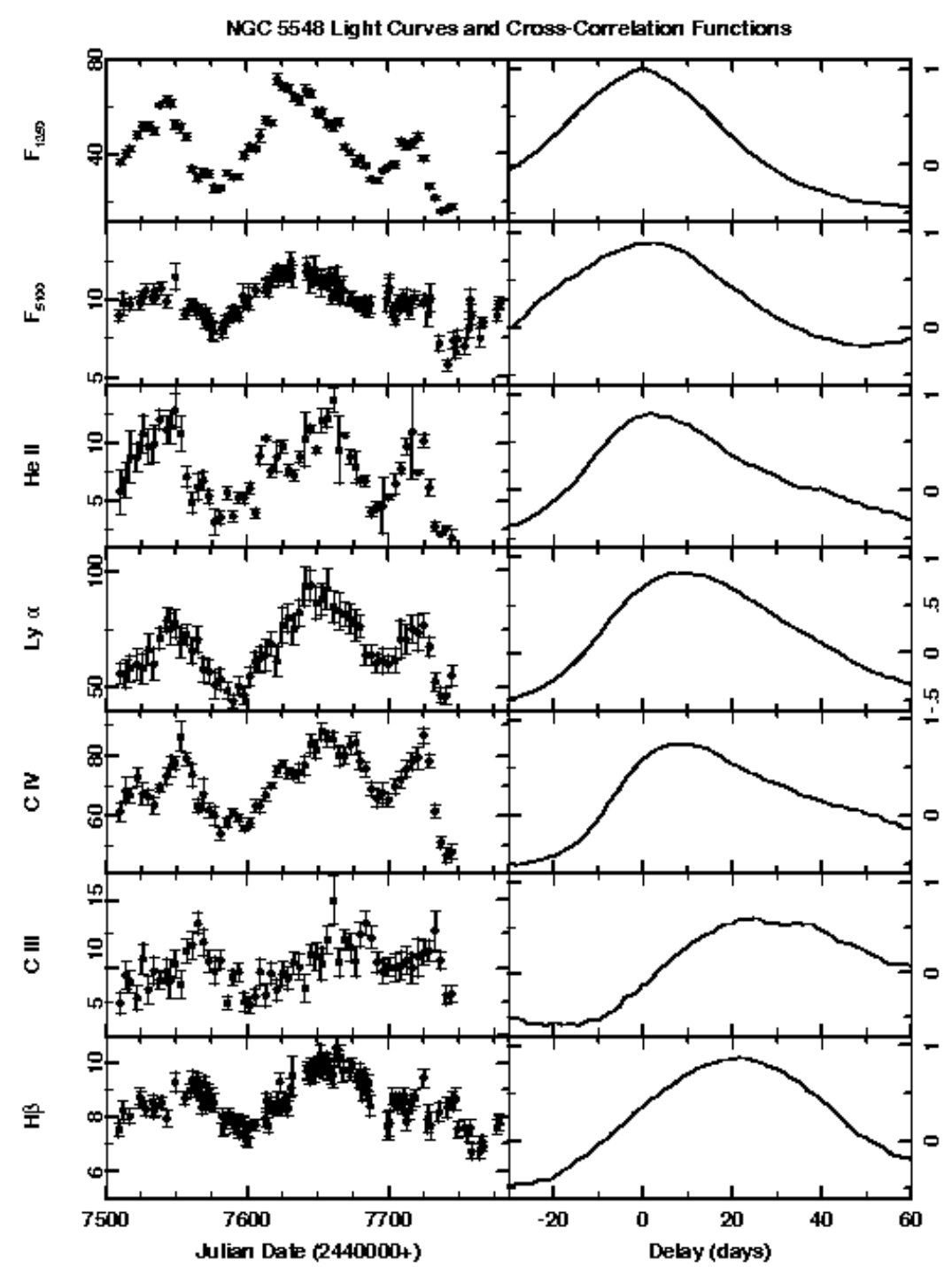

Reverberation Mapping Results

- Reverberation lags have been measured for ~50 AGNs, mostly for Hβ, but in some cases for multiple lines.
- AGNs with lags for multiple lines show that highest ionization emission lines respond most rapidly $\Rightarrow$ ionization stratification

NGC 5548 - 1989

Feature	F_{var}	Lag (days)
UV cont	0.321	…
Opt. Cont	0.117	$0.6^{+1.5}_{-1.5}$
He II λ1640	0.344	$3.8^{+1.7}_{-1.8}$
N V λ1240	0.441	$4.6^{+3.2}_{-2.7}$
He II λ4686	0.052	$7.8^{+3.2}_{-3.0}$
C IV λ1549	0.136	$9.8^{+1.9}_{-1.5}$
Lyα λ1215	0.169	$10.5^{+2.1}_{-1.9}$
Si IV λ1400	0.185	$12.3^{+3.4}_{-3.0}$
Hβ λ4861	0.091	$19.7^{+1.5}_{-1.5}$
C III] λ1909	0.130	$27.9^{+5.5}_{-5.3}$

BLR Scaling with Luminosity

- To first order, AGN spectra look the same

$$U = \frac{Q(\mathrm{H})}{4\pi r^2 n_\mathrm{H} c} \propto \frac{L}{n_\mathrm{H} r^2}$$

$\Rightarrow$ Same ionization parameter U

$\Rightarrow$ Same density n_H

$$r \propto L^{1/2}$$

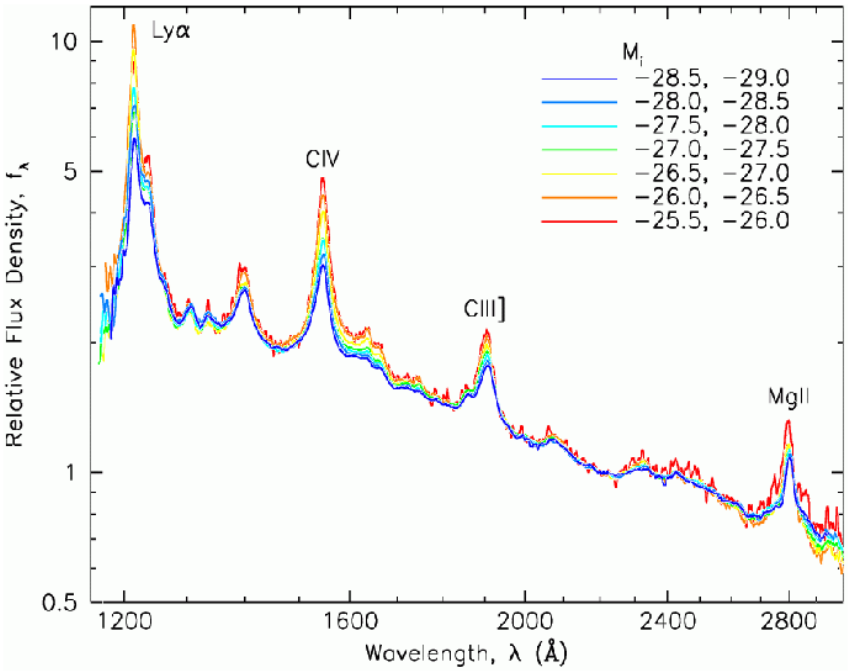

SDSS composites, by luminosity
Vanden Berk et al. (2004)

Scaling with Luminosity

- Importance of *R-L* relationship is that it is quicker way to estimate masses:

$$M_{\mathrm{BH}} \sim \Delta V^2 R / G \propto \Delta V^2 L^{1/2}$$

Detailed discussion in Lecture 3

BLR Radius-Luminosity Relationship

- $R \propto L^{½}$ relationship was anticipated long before it was well-measured.

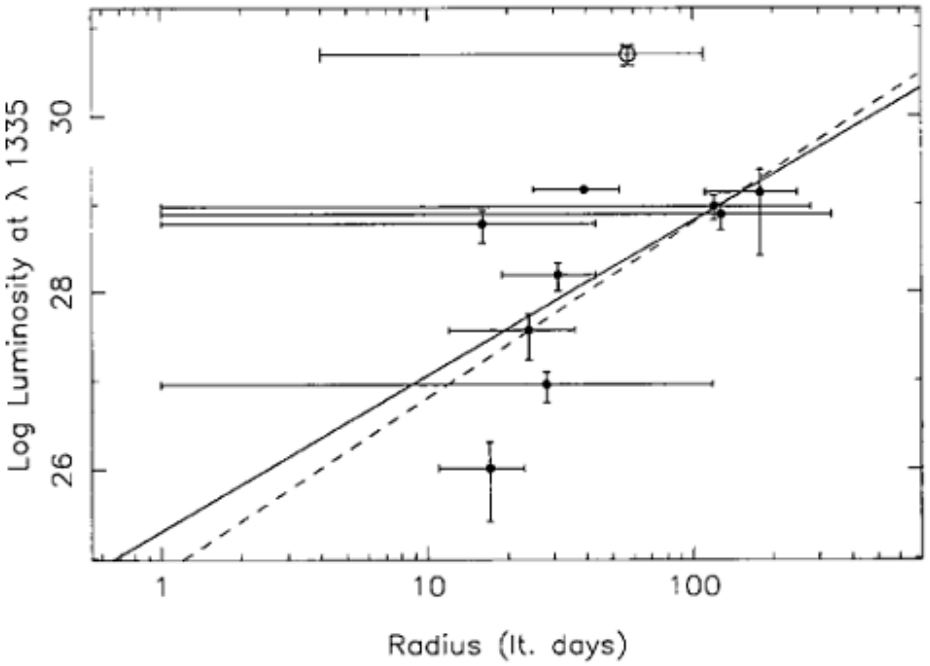

Koratkar & Gaskell 1991, ApJ, 370, L61

BLR Radius-Luminosity Relationship

- Kaspi et al. (2000) succeeded in observationally defining the *R-L* relationship
  - Increased luminosity range using PG quasars
  - PG quasars are bright compared to their hosts

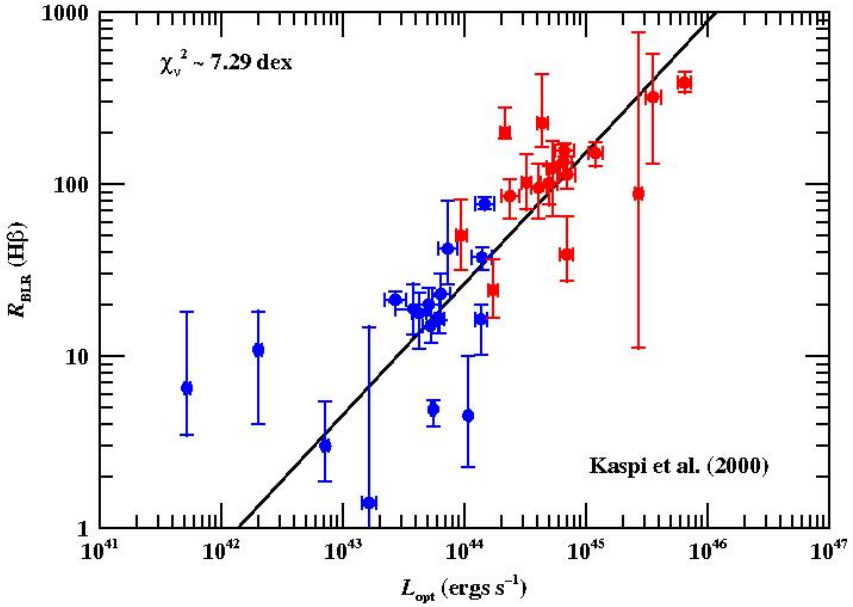

Kaspi+ 2000, ApJ, 533, 631

Progress in Determining the Radius-Luminosity Relationship

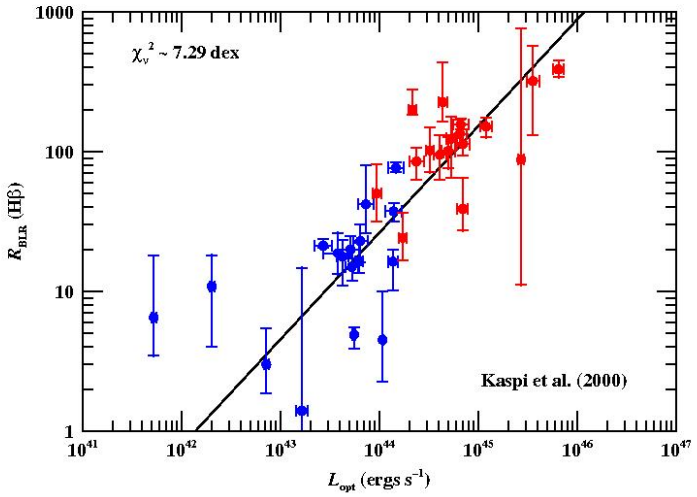

Original PG + Seyferts
(Kaspi et al. 2000)
$\chi_\nu^2 \approx 7.29$
$R(\mathrm{H}\beta) \propto L^{0.76}$

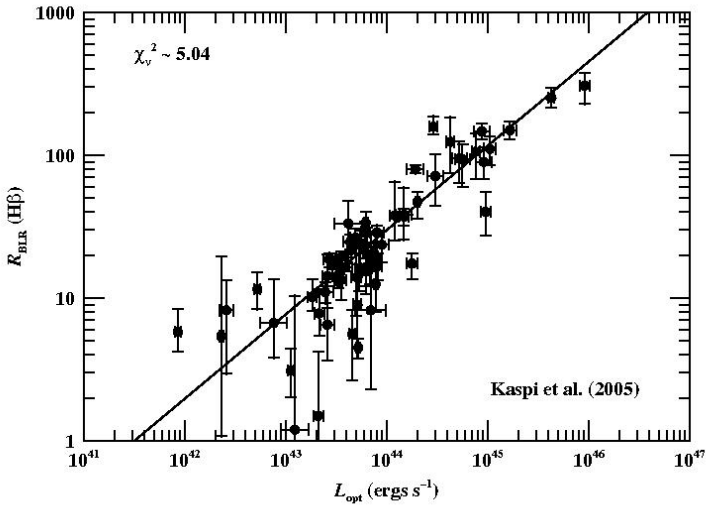

Expanded, reanalyzed
(Peterson et al. 2004;
Kaspi et al. 2005)
$\chi_\nu^2 \approx 5.04$
$R(\mathrm{H}\beta) \propto L^{0.59}$

NGC 4051
z = 0.00234
log L_{opt} = 41.8

Mrk 79
z =0.0222
log L_{opt} = 43.7

PG 0953+414
z = 0.234
log L_{opt} = 45.1

Reverberation experiments use large spectrograph apertures for accurate spectrophotometry.
This results in significant starlight contribution to the measured optical luminosity.

MDM images courtesy of M. Bentz

Aperture Geometries for Reverberation-Mapped AGNs

- Large apertures mitigate seeing effects.
- They also admit a lot of host galaxy starlight!

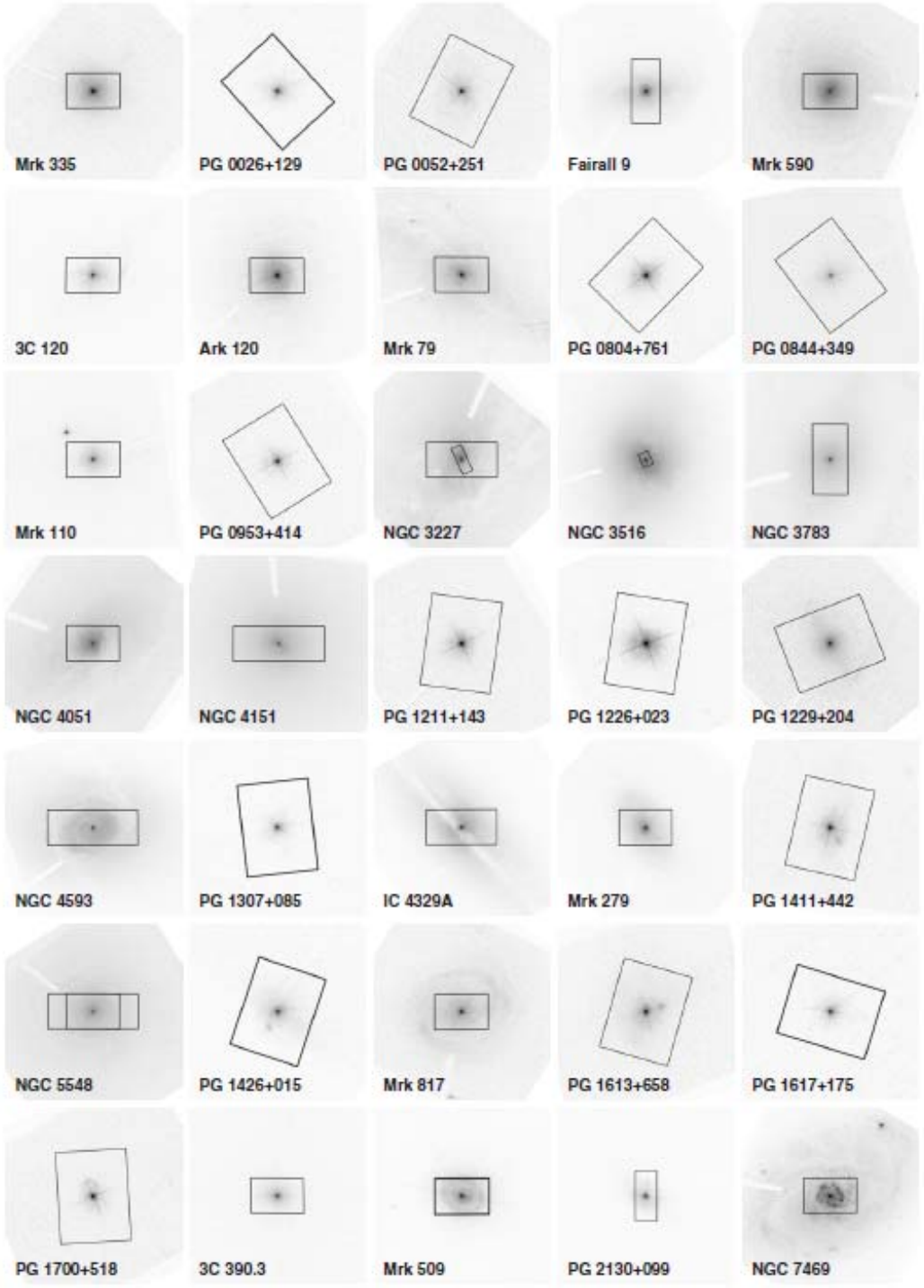

The *R*–*L* Relation

- Empirical slope ~0.55 ± 0.03
- Intrinsic scatter ~0.13 dex
- Typical error bars on best reverberation data ~0.09 dex
- Conclusion: for Hβ over the calibrated range ($42 \leq \log \lambda L_{5100}$ (ergs s^{-1}) ≤ 46 at $z \approx 0$), *R-L* is nearly as effective as reverberation.

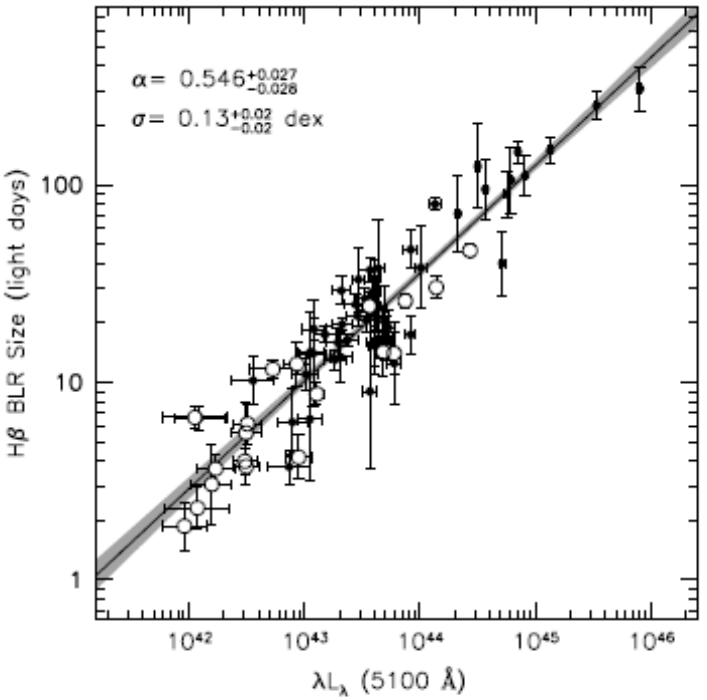

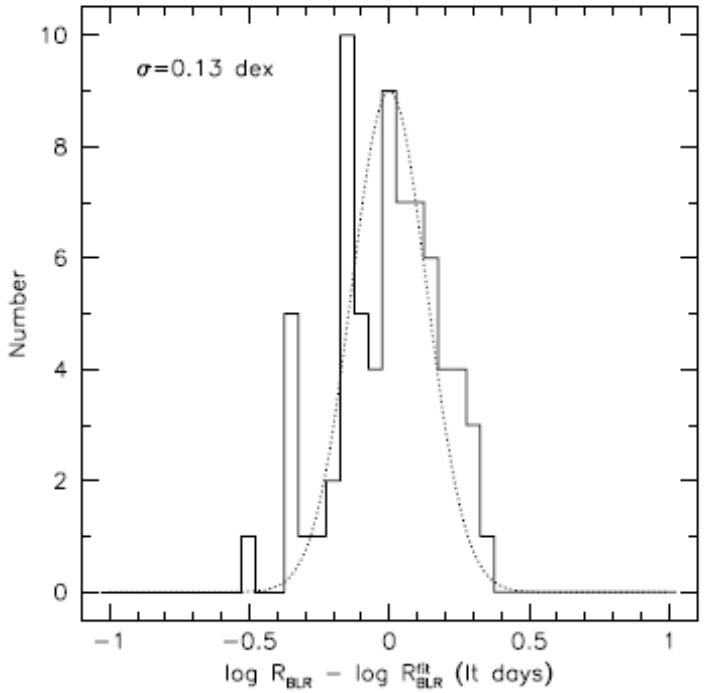

Bentz+ 2013, ApJ, 767:149

Independent confirmation of *R*–*L* from microlensing, including high-ionization lines.

RM measurements, low ionization lines

Microlensing, Low-ionization lines

RM measurements, high-ionization lines

Microlensing, high-ionization lines

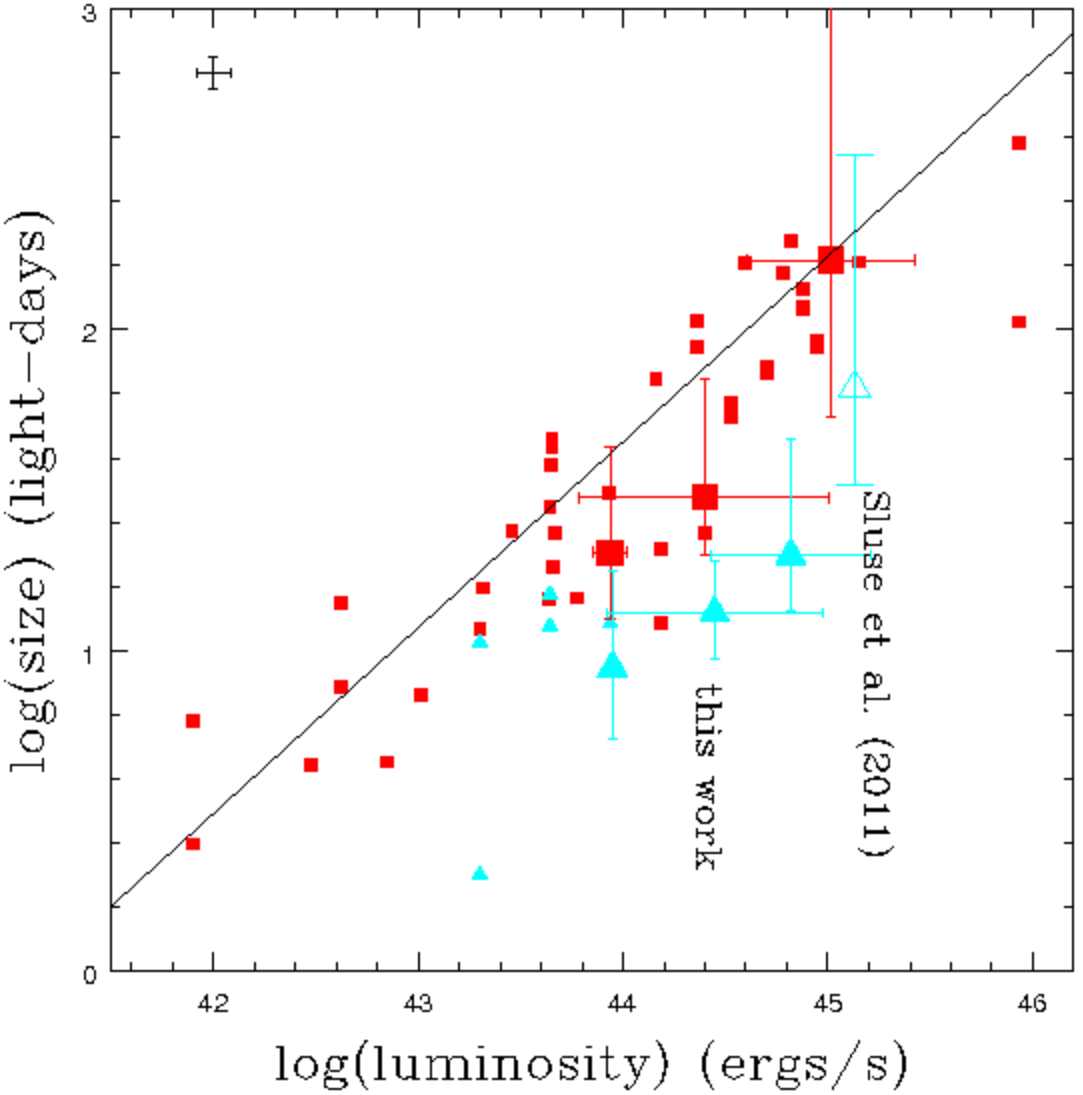

Guerras, Kochanek + 2013

BLR Size vs. Luminosity

- Should the same relationship should hold as a single object varies in luminosity?
- The Hβ response in NGC 5548 has been measured for ~16 individual observing seasons.
  - Measured lags range from 6 to 26 days
  - Best fit is $\tau \propto L_{opt}^{0.9}$

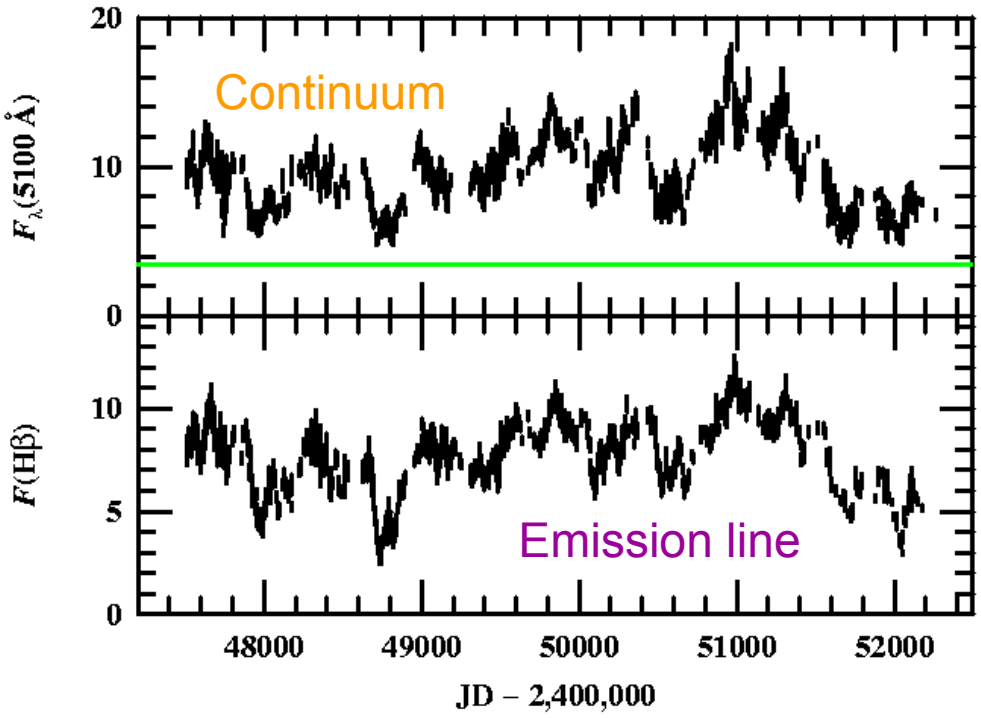

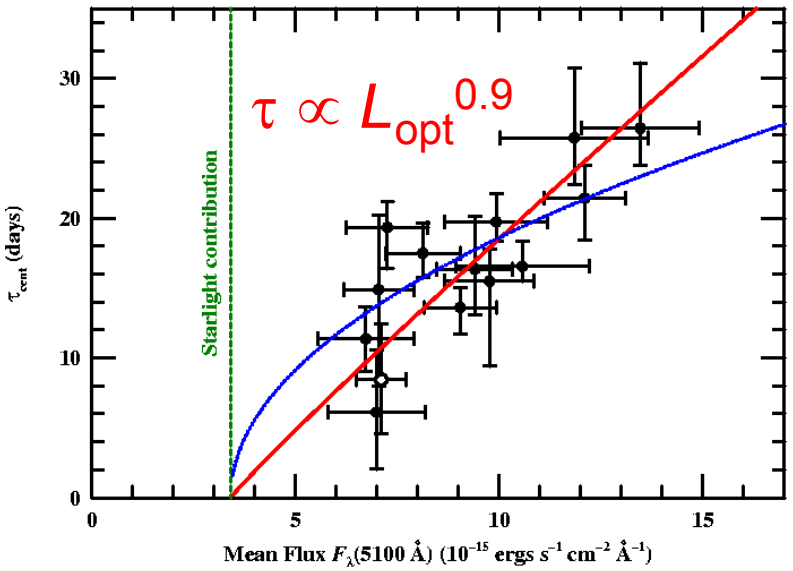

BLR Size vs. Luminosity

- However, UV varies with higher amplitude than than optical!

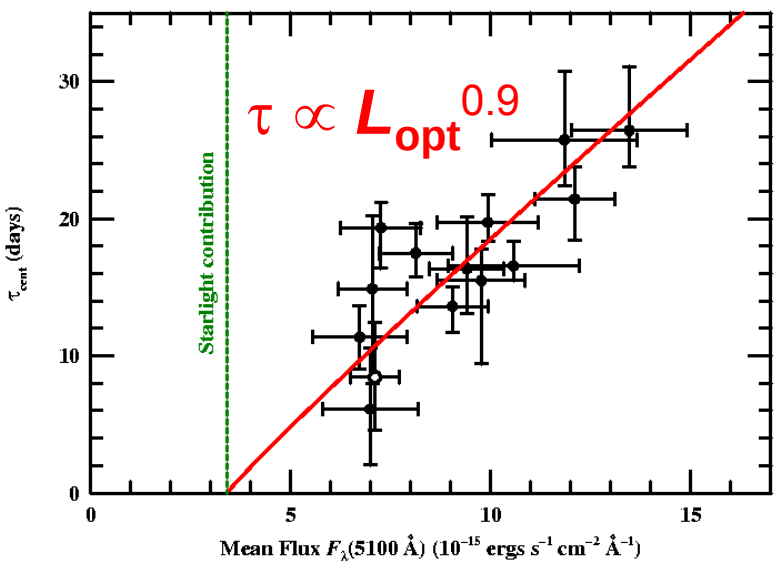

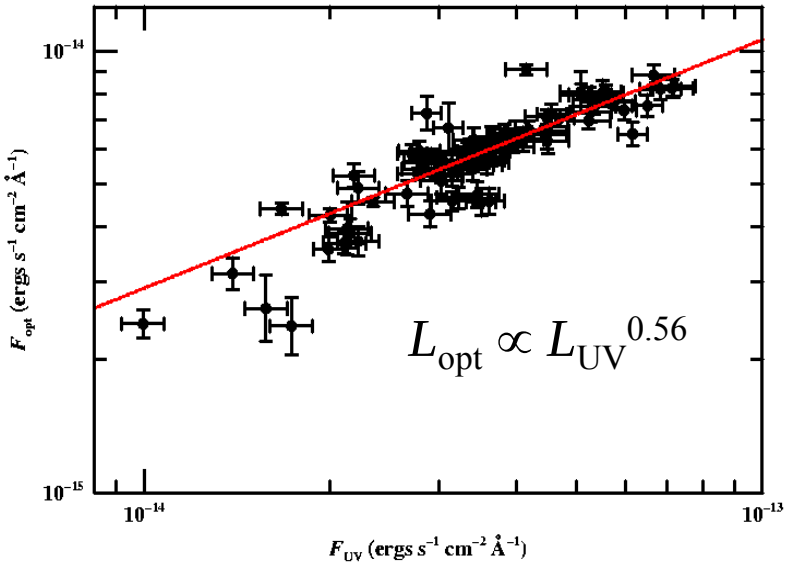

$$\tau \propto L_{opt}^{0.9} \propto (L_{UV}^{0.56})^{0.9} \propto L_{UV}^{0.5}$$

Again surprisingly consistent with the naïve prediction!

What Fine-Tunes the BLR?

- Why are the ionization parameter and electron density the same for all AGNs?
- How does the BLR know precisely where to be?
- *Answer:* gas is everywhere in the nuclear regions. We see emission lines emitted under optimal conditions.

Locally optimally-emitting cloud (LOC) model

- “Clouds” of various density are distributed throughout the nuclear region.
- Emission in a particular line comes predominantly from clouds with optimal conditions for that line.

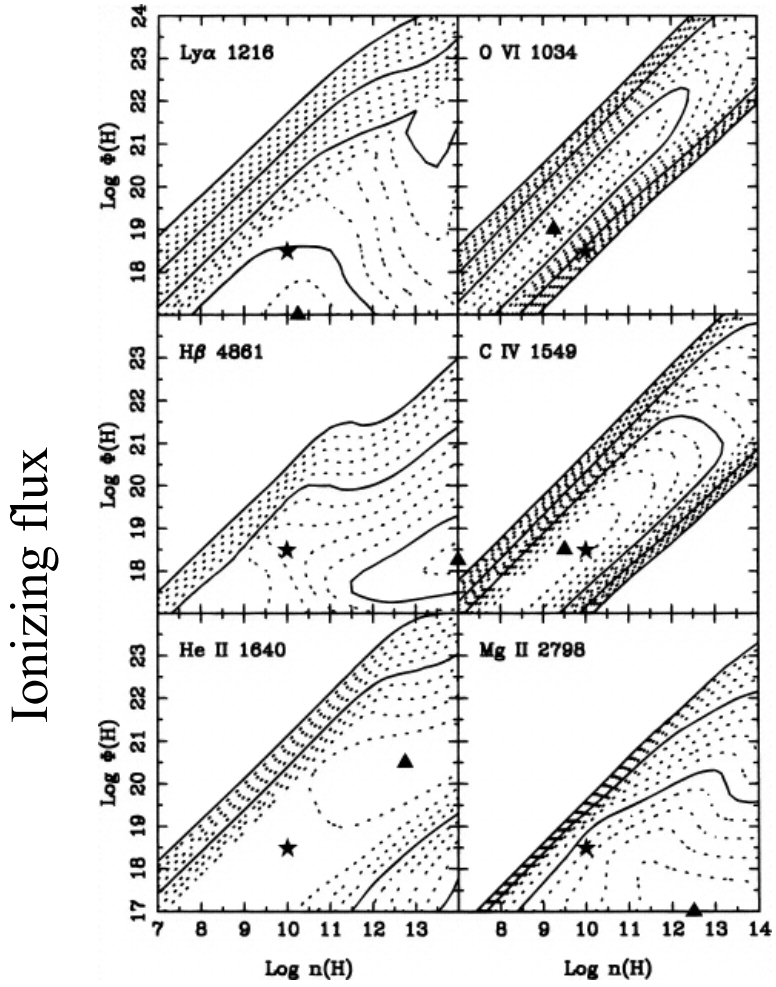

Korista et al. (1997)

Mass of the BLR

- Reverberation mapping + LOC model suggest that there is a large amount of mass in the BLR, most not emitting very efficiently.
- Baldwin et al. (2003) estimate total mass of BLR at 10^4 – 10^5 $M_\odot$

A Few Other Possibly Pertinent Observations…

- Line profile variability is not a reverberation effect.
  - Time scales are much longer than reverberation timescales
  - Reverberation signals are quite weak (AGN varies ~10-20% on reverberation timescales.

30 Years of NGC 5548

Hβ & Continuum Variability
1972–2002

Sergei Sergeev (CrAO)
Richard Pogge (OSU)
Bradley Peterson (OSU)

A Few Other Possibly Pertinent Observations…

- While line variations well-correlated with UV/optical, X-rays continuum shows more complex relationship with UV/optical.

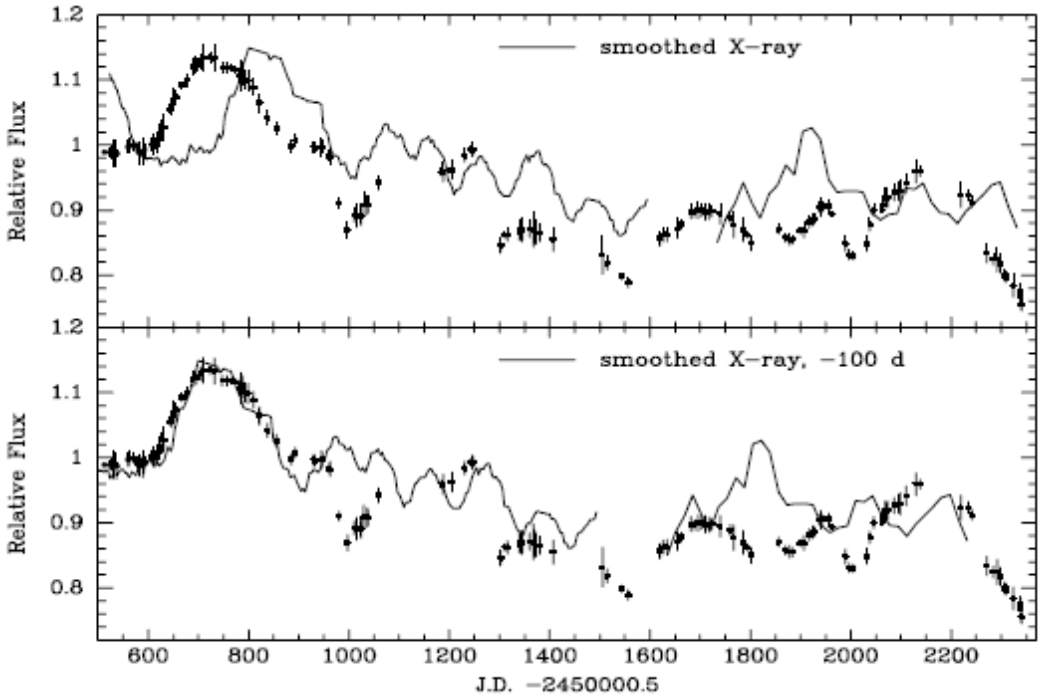

NGC 3783

Data points: *R*-band
Solid line: smoothed X-ray

Maoz+ 2002, AJ, 124, 1988

Highly Variable X-Ray Absorption

- Changes in absorption columns (~10^{23} cm^{-2}) on timescales of ~ 1 day or less.
  - Implied columns, transverse velocities, distance from central source point to BLR.

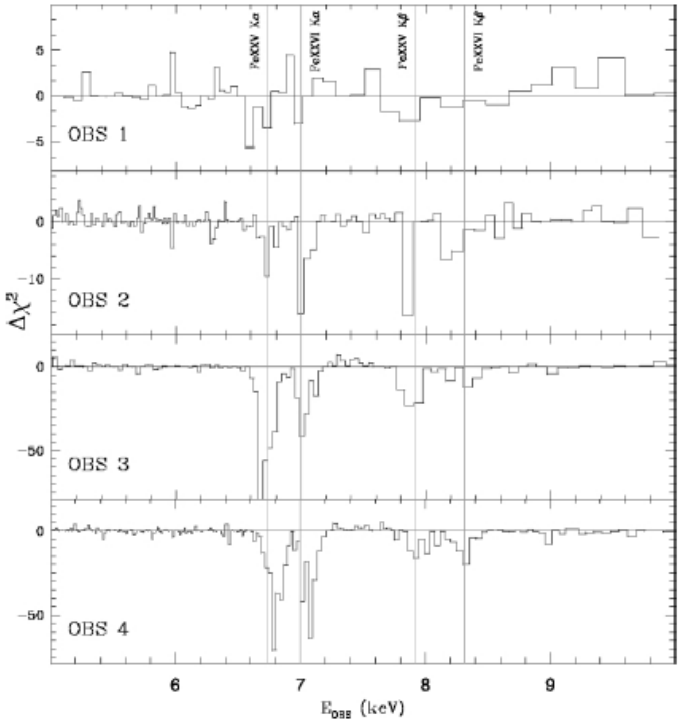

Risaliti et al. 2005

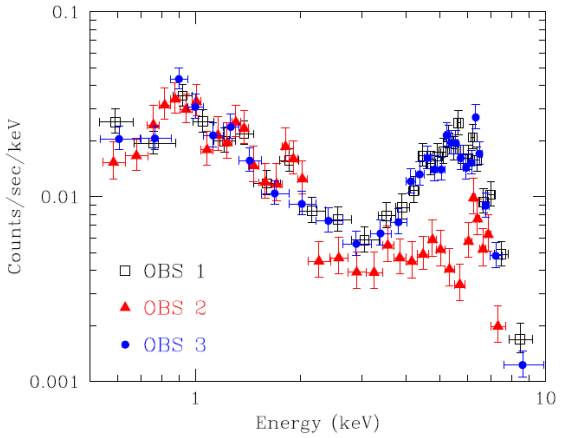

Risaliti 2007

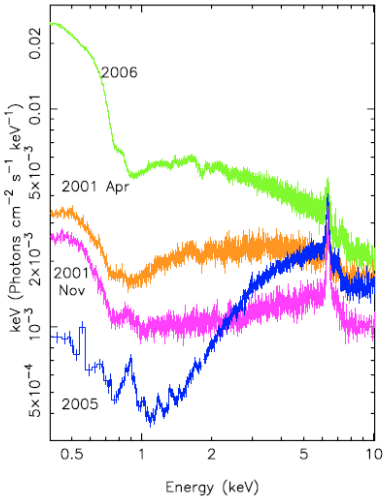

Turner et al. 2008

A Few Other Possibly Pertinent Observations…

- While Balmer lines appear to arise in infalling gas, there is evidence for outflow in the UV lines.

Outflow Component of the BLR

- Evidence for outflows
  - Blueshifted absorption features are common
  - Clear blueward asymmetries in some cases

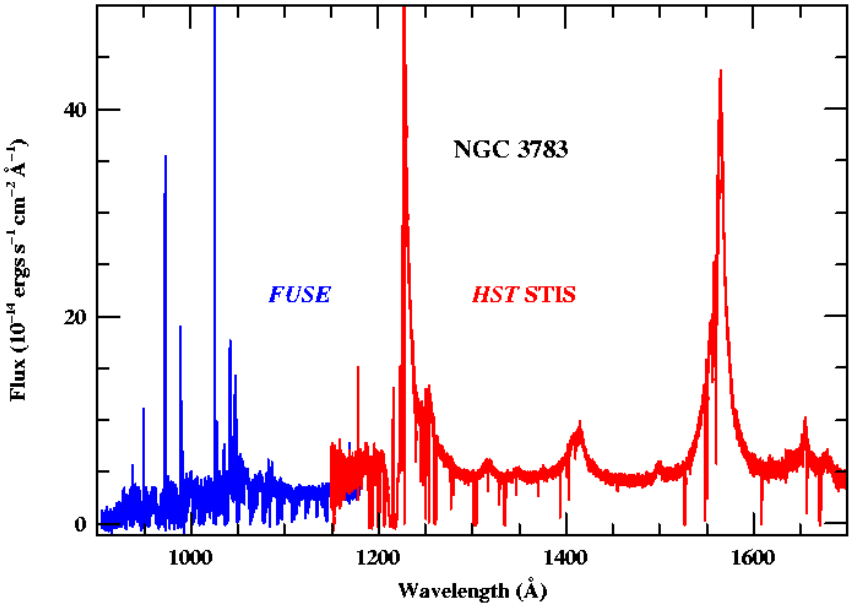

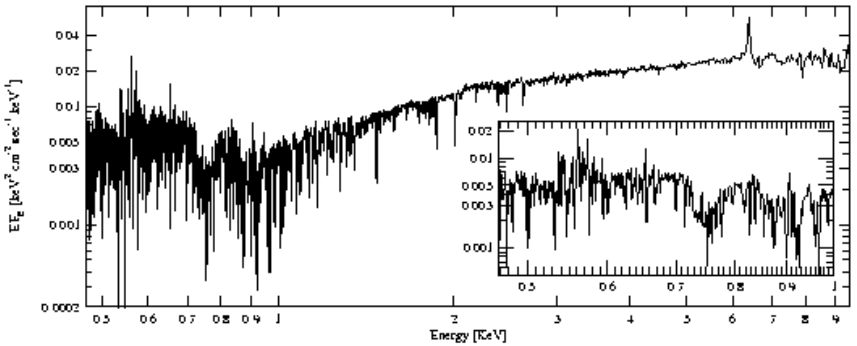

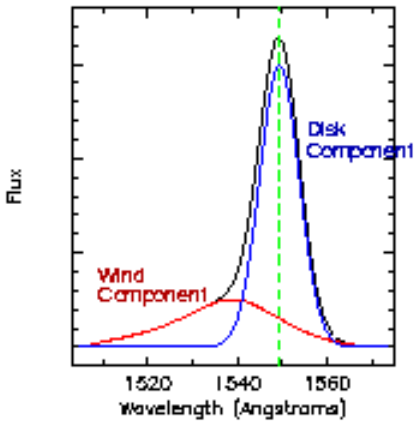

Leighly (2001)

Chandra: Kaspi et al. (2002)
HST: Crenshaw et al. (2002)
FUSE: Gabel et al. (2002)

Evidence for Outflows in AGNs

- Peaks of high ionization lines are blueshifted relative to systemic.
- Maximum blueshift increases with luminosity.

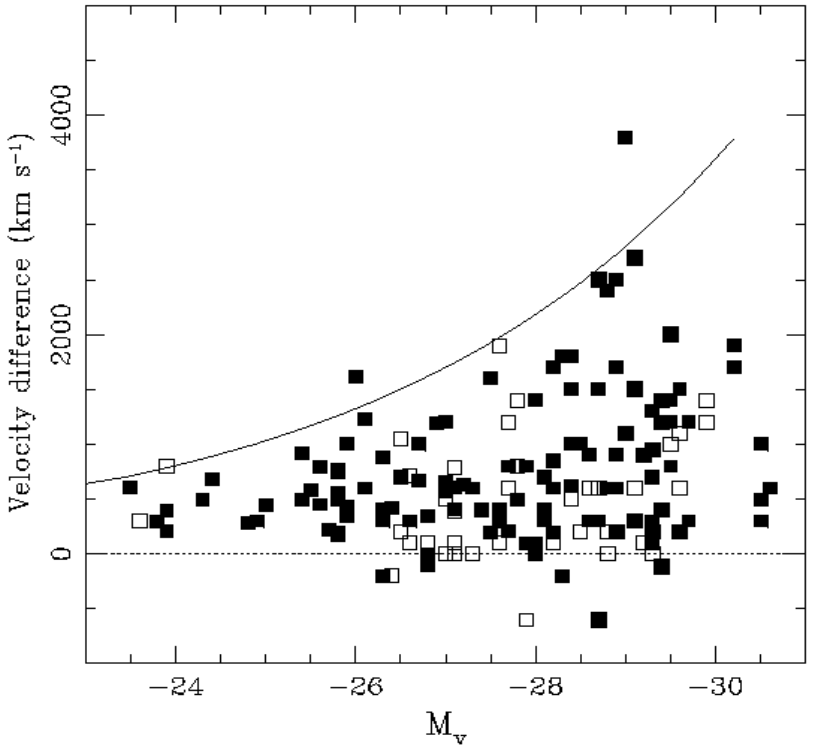

Espey (1997)

A Disk-Wind Concept

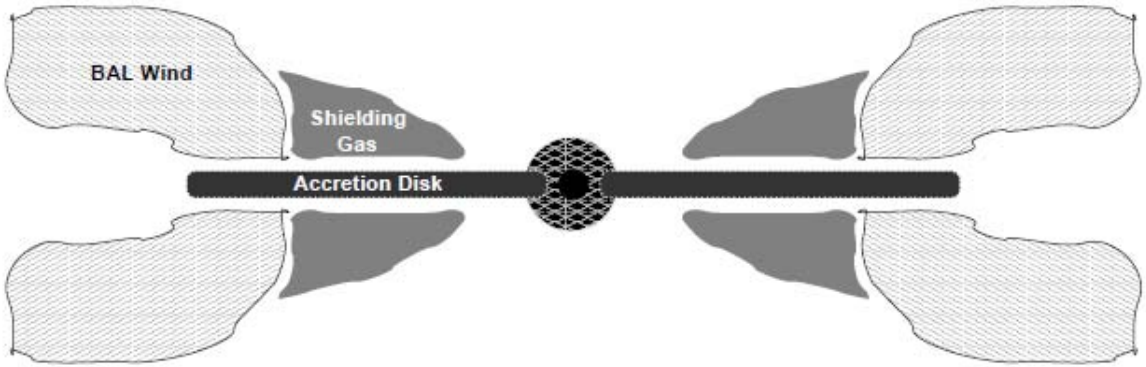

Gallagher et al. 2004

Wind could be hydromagnetical or radiation-pressure driven

- Theory: Murray & Chiang, Proga, Blandford & Payne
- Phenomenology: Elvis, S. Gallagher, Vestergaard

Summary Points

- Reverberation mapping is beginning to reveal the structure of the broad-line region in AGNs.
- There is a well-established relationship between the size of the broad-line region and the AGN luminosity.
- These will be important in Lecture 3